Heterodyne Detection of Axions in SRF Cavities

Sebastian A. R. Ellis

Université de Genève

***JHEP* 07 (2020) 088, hep-ph/1912.11048**
A. Berlin, R. T. D'Agnolo, **SARE,** P. Schuster, N. Toro,
C. Nantista, J. Neilson, S. Tantawi, K. Zhou

***PRD* 104 (2021) 11, L111701, hep-ph/2007.15656**
A. Berlin, R. T. D'Agnolo, **SARE,** K. Zhou

High-level Summary

Search for weakly-coupled signals in a *loaded* SRF cavity

Oscillating background B-field: **heterodyne up-conversion approach decouples axion m_a from V_{det}**

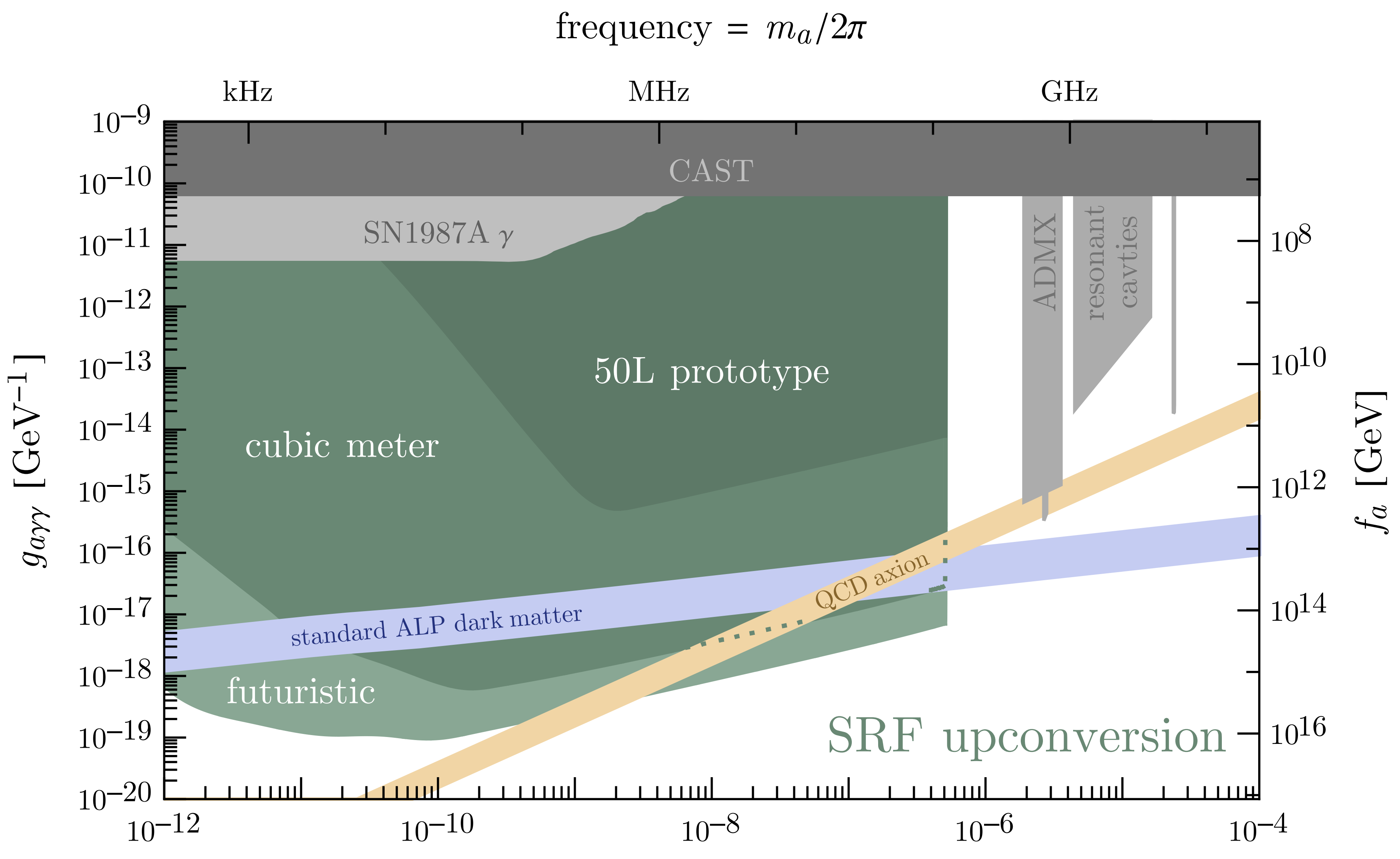

$$\mathcal{L}_{\text{in}} \sim -g_{a\gamma\gamma} a F \tilde{F}$$

$$\omega_{\text{sig}} = \omega_0 \pm \omega_{\text{in}}$$

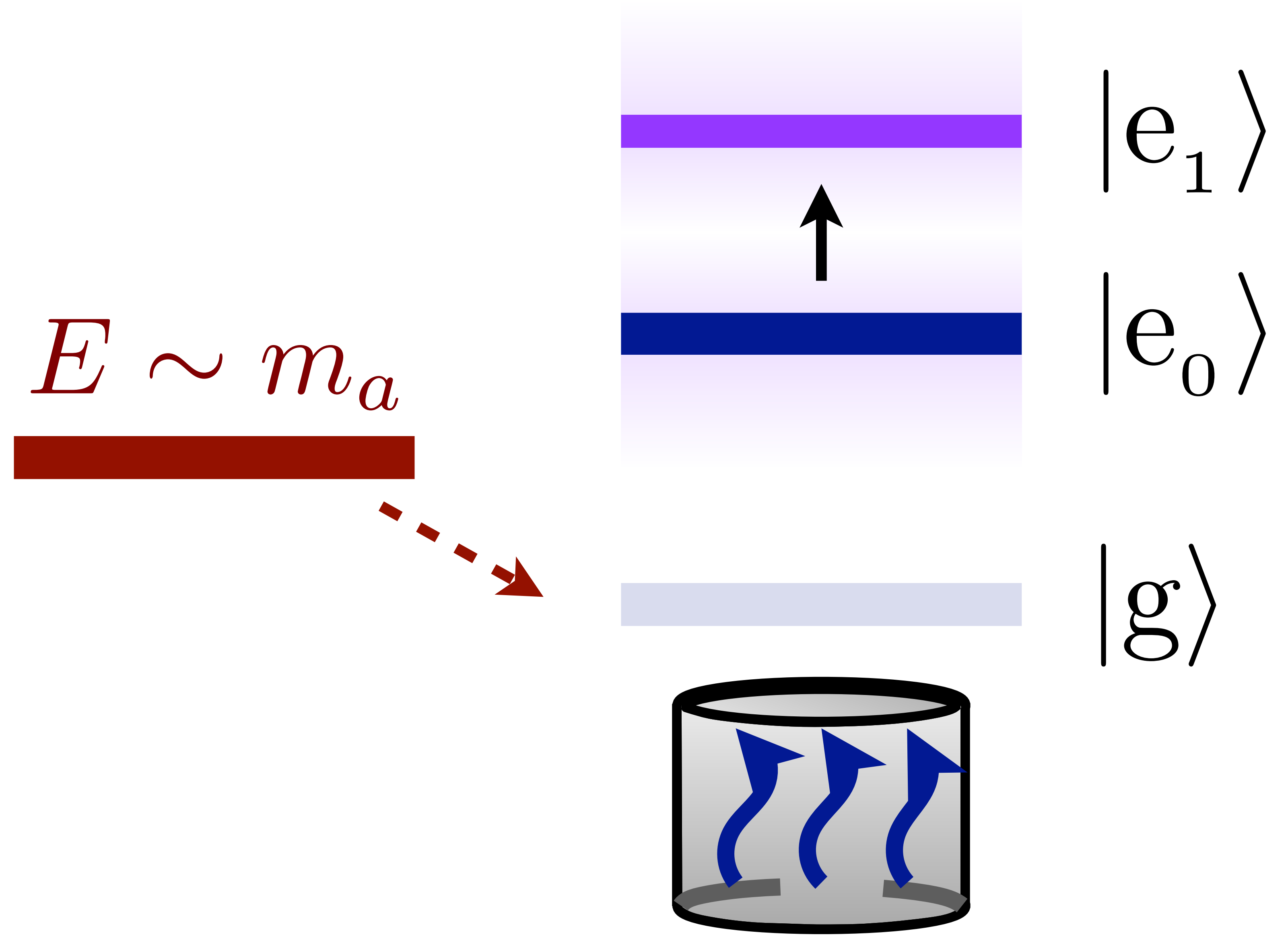

***Oscillating B*-field in a box**

Axion, ALPs and Axion Electrodynamics

Axion introduced to solve strong CP problem

$$\mathcal{L} \supset \left(\frac{a}{f_a} + \bar{\theta}\right) \frac{g_s^2}{32\pi^2} G^a_{\mu\nu}\tilde{G}^{\mu\nu,a}$$

Peccei & Quinn (1977)
Weinberg (1978)
Wilczek (1978)

$$d_n \sim 10^{-16}\bar{\theta}\ e\ \mathrm{cm}$$

$$d_n^{\mathrm{exp}} \lesssim 10^{-26}\ e\ \mathrm{cm}$$

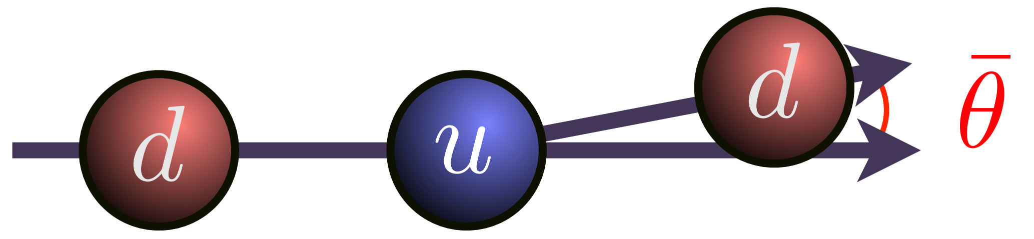

Axion, ALPs and Axion Electrodynamics

Axion introduced to solve strong CP problem

$$\mathcal{L} \supset \left(\frac{a}{f_a} + \bar{\theta}\right) \frac{g_s^2}{32\pi^2} G^a_{\mu\nu} \tilde{G}^{\mu\nu,a}$$

Peccei & Quinn (1977)
Weinberg (1978)
Wilczek (1978)

$$d_n \sim 10^{-16} \bar{\theta} \; e \text{ cm}$$

$$d_n^{\text{exp}} \lesssim 10^{-26} \; e \text{ cm}$$

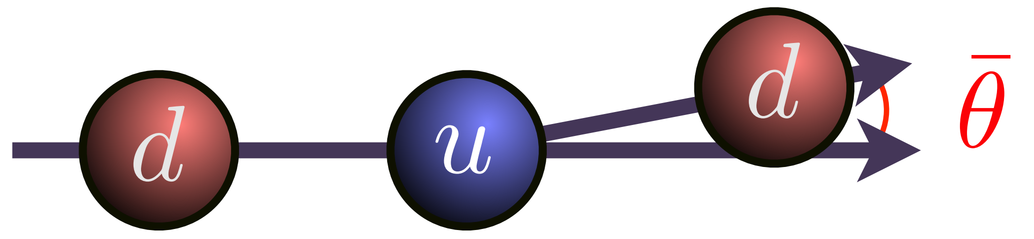

Mixing w/ pion or from full theory:

$$\mathcal{L} \supset -\frac{g_{a\gamma\gamma}}{4} \, a \, F \tilde{F} = -g_{a\gamma\gamma} \, a \, \mathbf{E} \cdot \mathbf{B}$$

Axion, ALPs and Axion Electrodynamics

Axion introduced to solve strong CP problem

$$\mathcal{L} \supset \left(\frac{a}{f_a} + \bar{\theta}\right) \frac{g_s^2}{32\pi^2} G^a_{\mu\nu}\tilde{G}^{\mu\nu,a}$$

Peccei & Quinn (1977)
Weinberg (1978)
Wilczek (1978)

$$d_n \sim 10^{-16}\bar{\theta}\; e\text{ cm}$$
$$d_n^{\text{exp}} \lesssim 10^{-26}\; e\text{ cm}$$

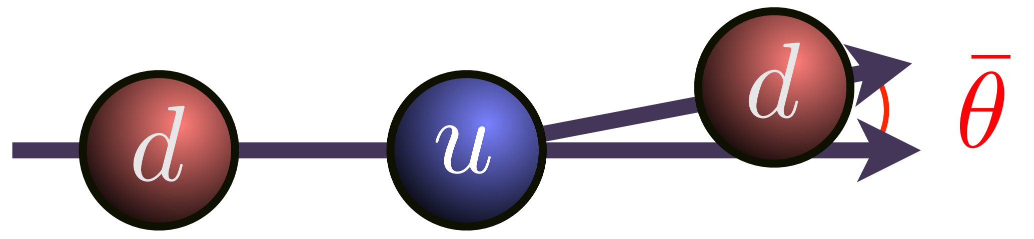

Mixing w/ pion or from full theory:

$$\mathcal{L} \supset -\frac{g_{a\gamma\gamma}}{4}\, a\, F\tilde{F} = -g_{a\gamma\gamma}\, a\, \mathbf{E}\cdot\mathbf{B}$$

$$\nabla\cdot\mathbf{E} = \rho - g_{a\gamma\gamma}\mathbf{B}\cdot\nabla a$$
$$\nabla\times\mathbf{B} = \partial_t\mathbf{E} + \mathbf{J} - g_{a\gamma\gamma}\left(\mathbf{E}\times\nabla a - \mathbf{B}\partial_t a\right)$$

Maxwell's new and improved Equations

Axion, ALPs and Axion Electrodynamics

Axions as dark matter:

$$a(t) \simeq \frac{\sqrt{2\rho_{\rm DM}}}{m_a} \cos\left(m_a t + m_a \boldsymbol{v}\cdot\boldsymbol{x} + \varphi\right)$$

$$v \sim 10^{-3}\, c$$

Axion, ALPs and Axion Electrodynamics

Axions as dark matter:

$$a(t) \simeq \frac{\sqrt{2\rho_{\rm DM}}}{m_a} \cos\left(m_a t + m_a \boldsymbol{v}\cdot\boldsymbol{x} + \varphi\right)$$

$$v \sim 10^{-3}\, c$$

Cavity Equations of Motion:

$$(\nabla^2 - \partial_t^2)\boldsymbol{E}_1 = -g_{a\gamma\gamma}\left(\nabla\left(\boldsymbol{B}_0\cdot\nabla a\right) + \partial_t\left(\boldsymbol{E}_0\times\nabla a - \partial_t a\,\boldsymbol{B}_0\right)\right)$$

$$(\nabla^2 - \partial_t^2)\boldsymbol{B}_1 = g_{a\gamma\gamma}\nabla\times\left(\boldsymbol{E}_0\times\nabla a - \partial_t a\,\boldsymbol{B}_0\right)$$

Axion, ALPs and Axion Electrodynamics

Axions as dark matter:

$$a(t) \simeq \frac{\sqrt{2\rho_{\rm DM}}}{m_a} \cos\left(m_a t + m_a \boldsymbol{v}\cdot\boldsymbol{x} + \varphi\right) \qquad v \sim 10^{-3}\, c$$

Cavity Equations of Motion:

$$(\nabla^2 - \partial_t^2)\boldsymbol{E}_1 = -g_{a\gamma\gamma}\left(\nabla\left(\boldsymbol{B}_0\cdot\nabla a\right) + \partial_t\left(\boldsymbol{E}_0 \times \nabla a - \partial_t a\,\boldsymbol{B}_0\right)\right)$$

$$(\nabla^2 - \partial_t^2)\boldsymbol{B}_1 = g_{a\gamma\gamma}\nabla\times\left(\boldsymbol{E}_0 \times \nabla a - \partial_t a\,\boldsymbol{B}_0\right)$$

Axions and Cavities

FoM:

$$P_{\rm sig} \sim \omega_{\rm sig}^2 B_a^2 V \min\left(\frac{1}{\Delta\omega_r}, \frac{1}{\Delta\omega_a}\right)$$

and/or

$$\mathcal{R} \sim \frac{\Delta\omega_r}{t_{\rm int}} {\rm SNR}^2$$

Axions and Cavities

FoM:

$$P_{\rm sig} \sim \omega_{\rm sig}^2 B_a^2\, V \min\left(\frac{1}{\Delta\omega_r}, \frac{1}{\Delta\omega_a}\right)$$

and/or $$\mathcal{R} \sim \frac{\Delta\omega_r}{t_{\rm int}} \mathrm{SNR}^2$$

Maximise: $\omega_{\rm sig}\,,\, B_a,\, V$

Axions and Cavities

FoM:

$$P_{\mathrm{sig}} \sim \omega_{\mathrm{sig}}^2 B_a^2 V \min\left(\frac{1}{\Delta\omega_r}, \frac{1}{\Delta\omega_a}\right)$$

and/or $$\mathcal{R} \sim \frac{\Delta\omega_r}{t_{\mathrm{int}}}\mathrm{SNR}^2$$

Maximise: ω_{sig}, B_a, V

Minimise: P_{n}

Axions and Cavities

FoM:

$$P_{\rm sig} \sim \omega_{\rm sig}^2 B_a^2 V \min\left(\frac{1}{\Delta\omega_r}, \frac{1}{\Delta\omega_a}\right)$$

and/or $$\mathcal{R} \sim \frac{\Delta\omega_r}{t_{\rm int}} \mathrm{SNR}^2$$

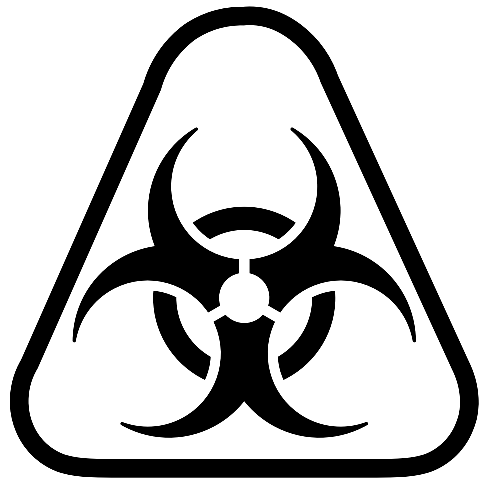

Maximise: $\omega_{\rm sig}$, B_a, V

Minimise: $P_{\rm n}$

Existing Approaches

Static-field Haloscope:
e.g. ADMX/RADES

$$\omega_{\text{sig}} = m_a \sim V^{-1/3}$$

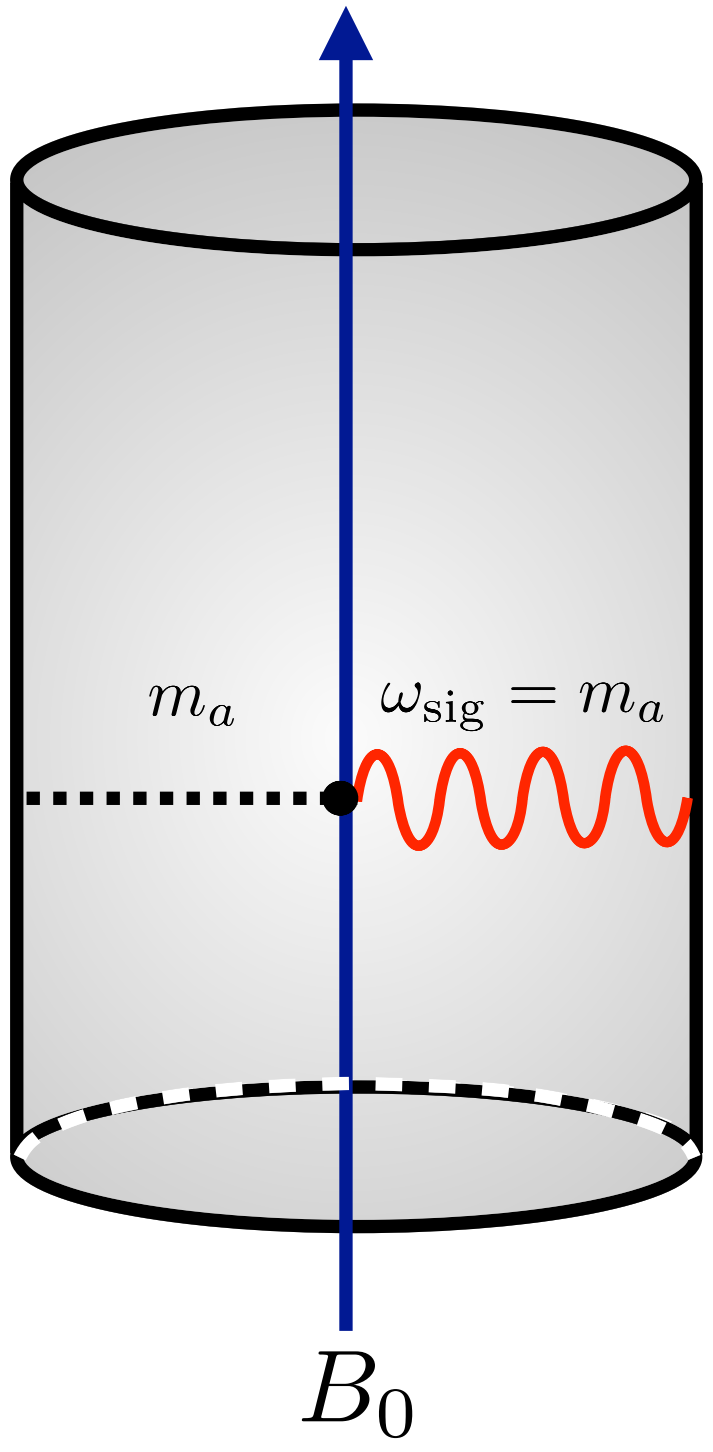

Existing Approaches

Static-field Haloscope:
e.g. ADMX/RADES

$$\omega_{\text{sig}} = m_a \sim V^{-1/3}$$

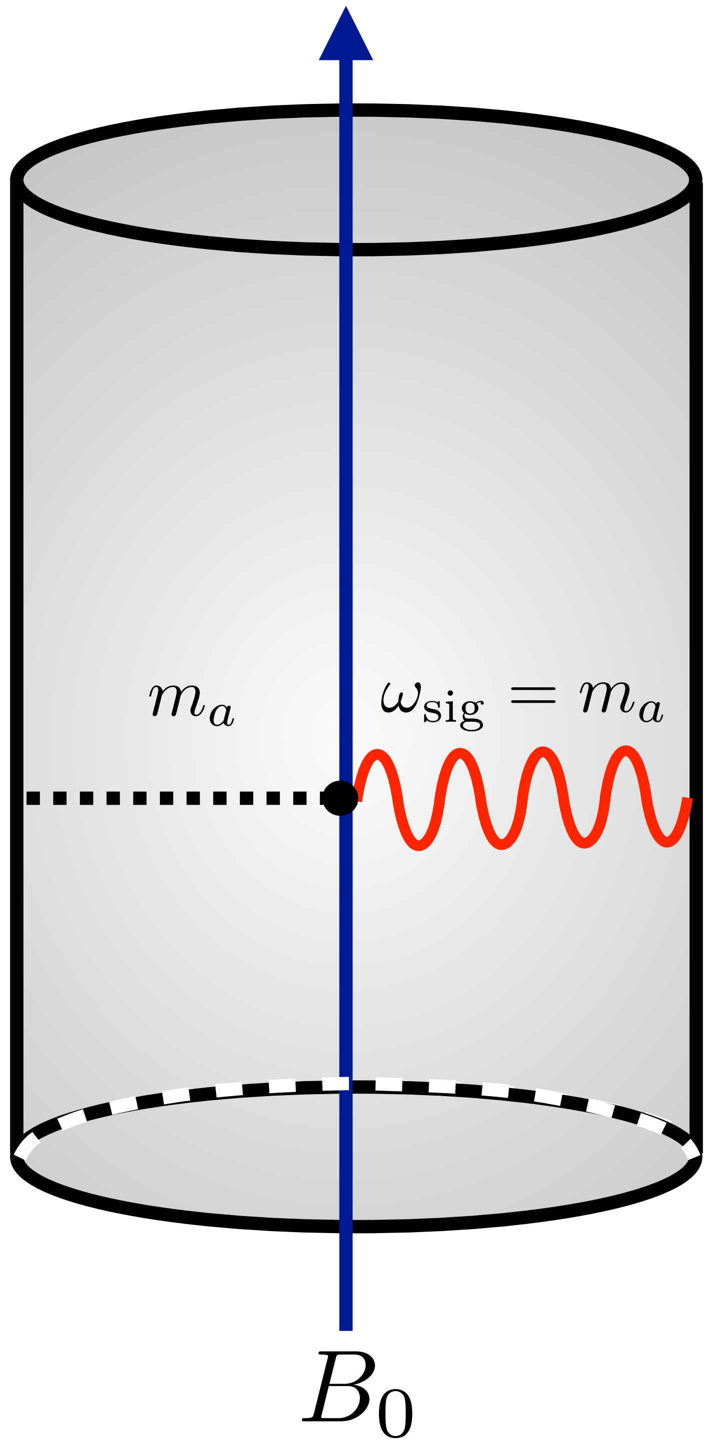

LC Resonator:
e.g. DM Radio

$$\omega_{\text{sig}} = m_a = \omega_{\text{LC}}$$

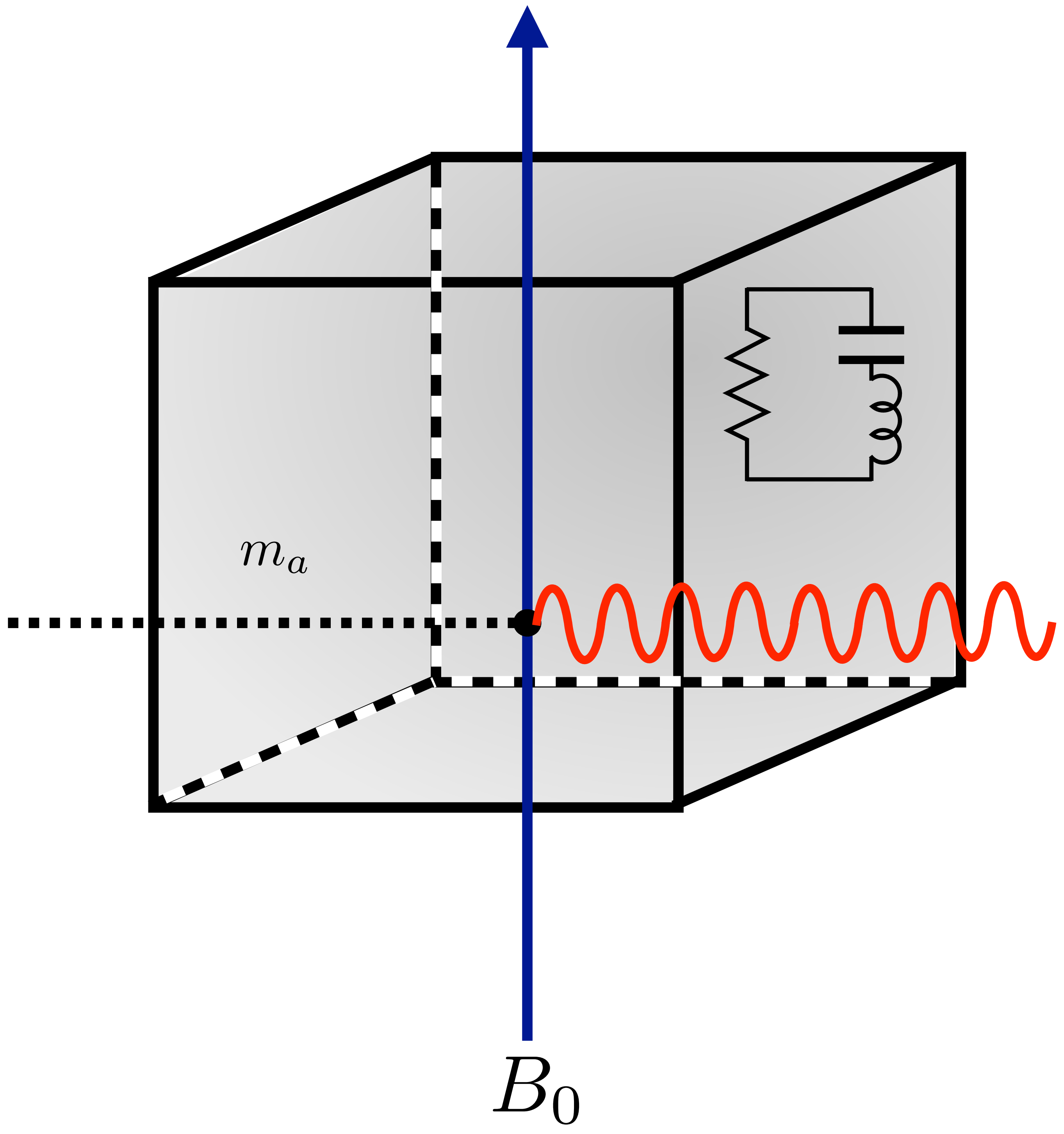

Existing Approaches

Static-field Haloscope:
e.g. ADMX/RADES

$$\omega_{\rm sig} = m_a \sim V^{-1/3}$$

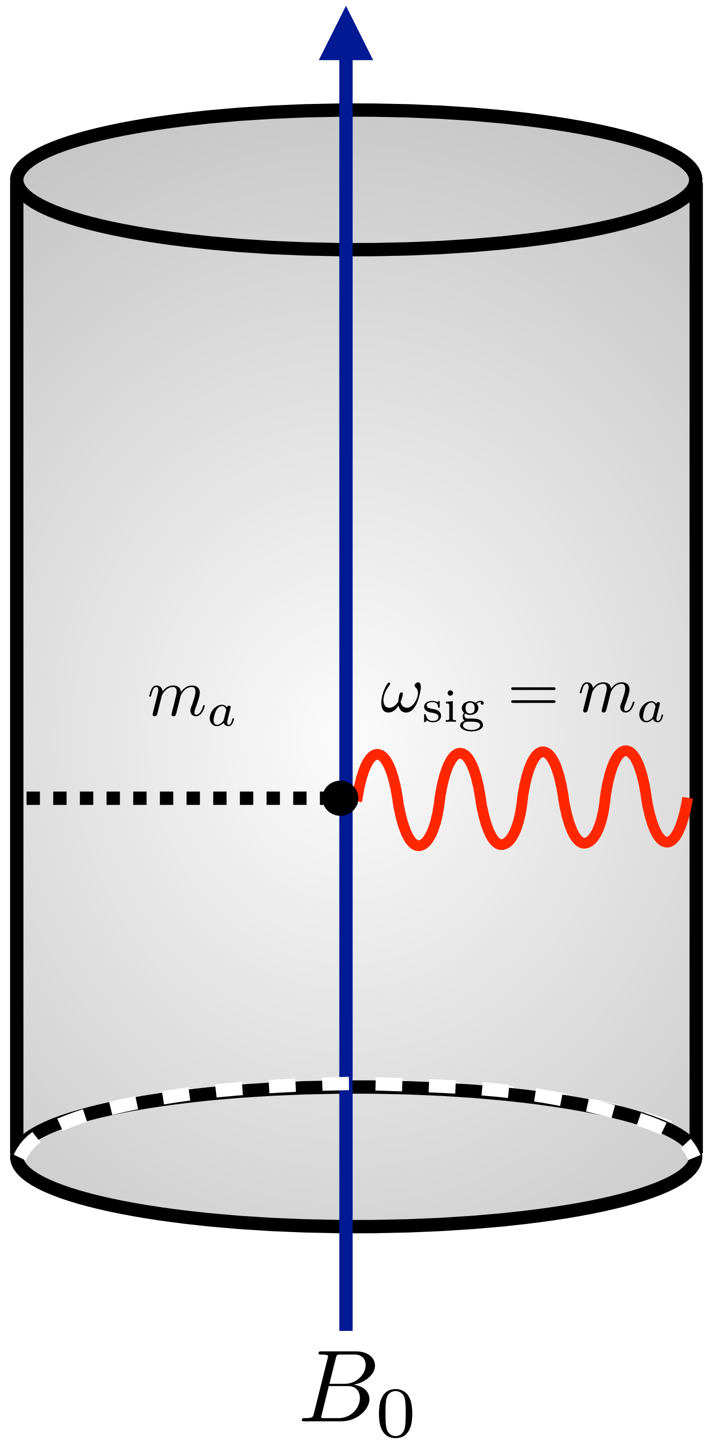

LC Resonator:
e.g. DM Radio

$$\omega_{\rm sig} = m_a = \omega_{\rm LC}$$

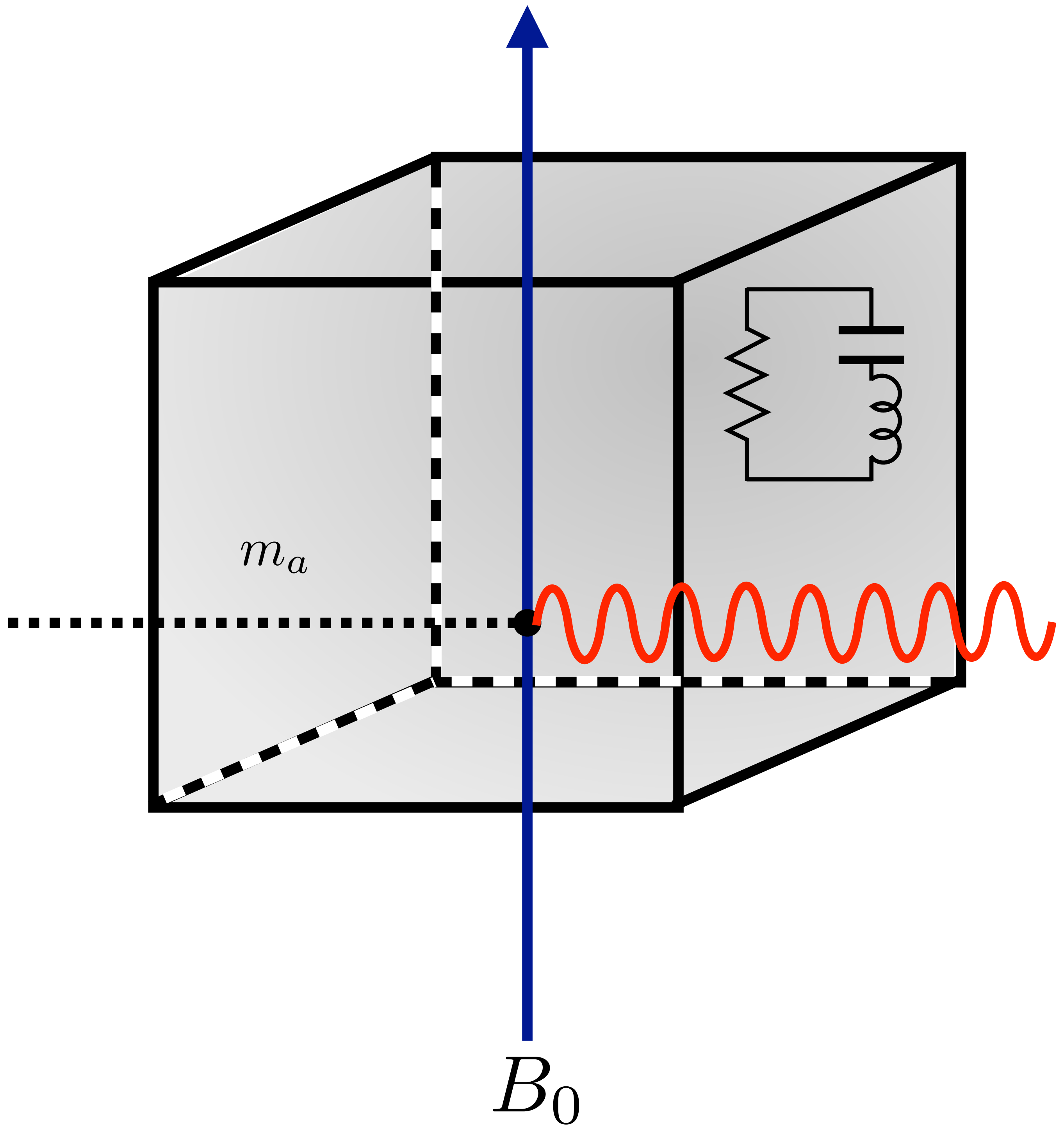

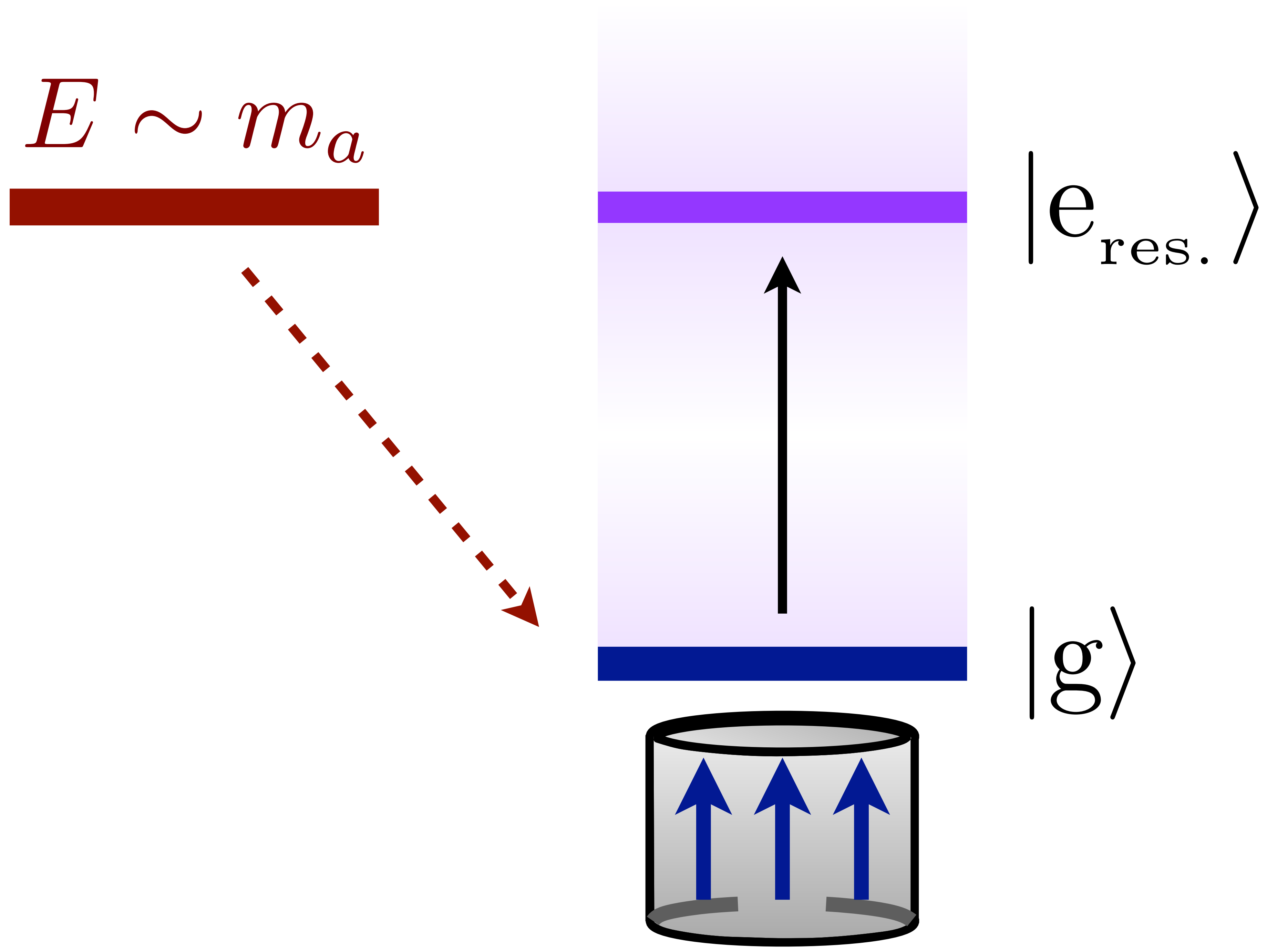

***B*-field in a box**

New Approach

Heterodyne Superconducting Radio-Frequency Resonator:

$$\omega_{\rm sig} \sim \omega_0 \pm m_a \sim V^{-1/3}$$

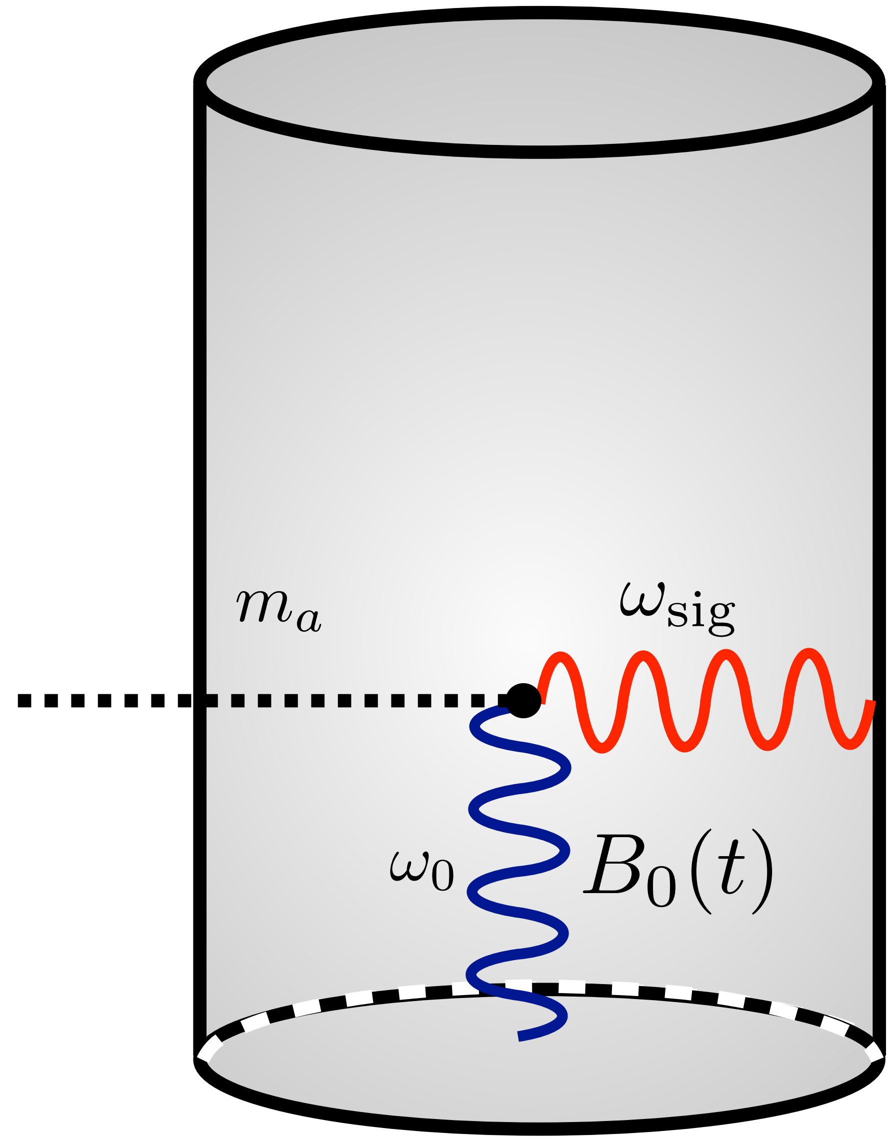

Enhances $\omega_{\rm sig}$

***JHEP* 07 (2020) 088, hep-ph/1912.11048**
A. Berlin, R. T. D'Agnolo, **SARE,** P. Schuster, N. Toro, C. Nantista, J. Neilson, S. Tantawi, K. Zhou

***PRD* 104 (2021) 11, L111701, hep-ph/2007.15656**
A. Berlin, R. T. D'Agnolo, **SARE,** K. Zhou

Decouples axion mass from detector volume

New Approach

Heterodyne Superconducting Radio-Frequency Resonator:

Q-factor $\gtrsim 10^{10}$

Applications elsewhere,
e.g. Quantum Computing:
see e.g. quant-ph/2304.09345

Enhances B_a

$$\omega_{\rm sig} \sim \omega_0 \pm m_a \sim V^{-1/3}$$

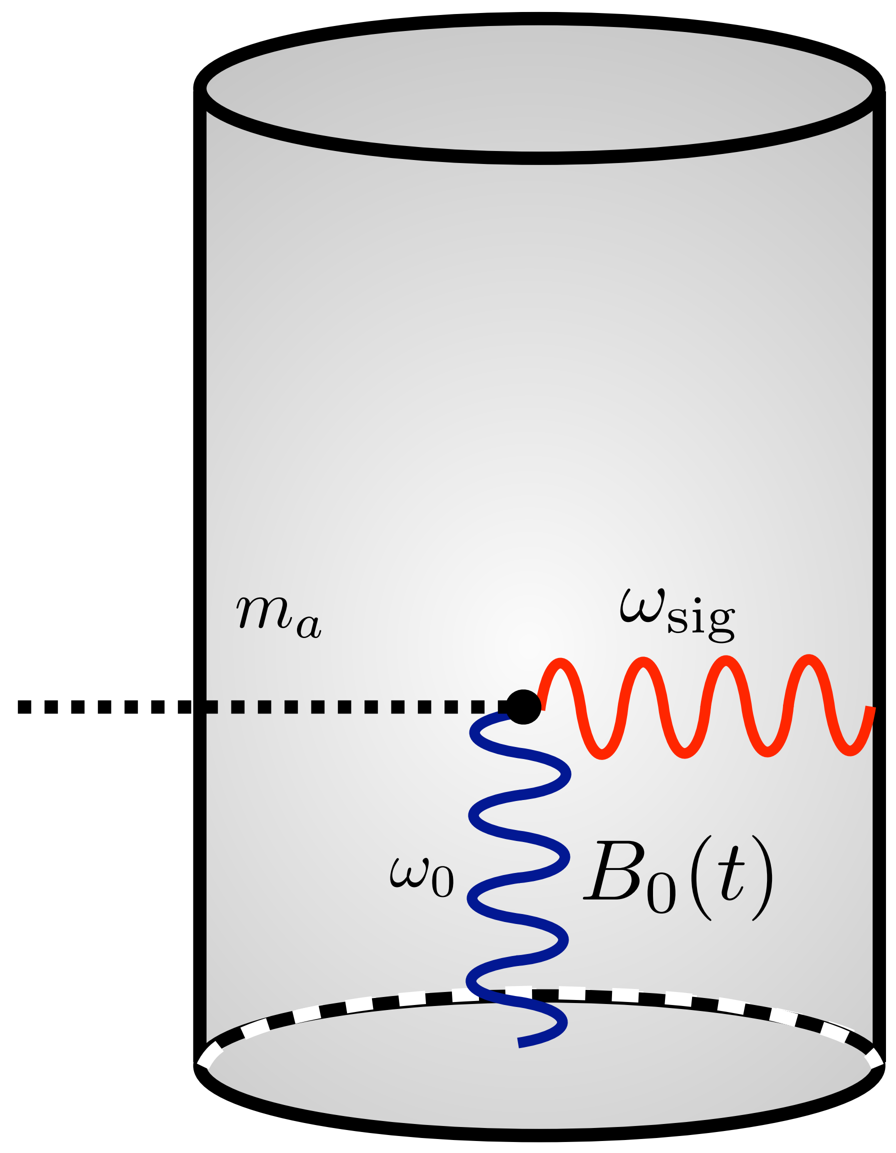

Enhances $\omega_{\rm sig}$

***JHEP* 07 (2020) 088, hep-ph/1912.11048**
A. Berlin, R. T. D'Agnolo, **SARE,** P. Schuster, N. Toro, C. Nantista, J. Neilson, S. Tantawi, K. Zhou

***PRD* 104 (2021) 11, L111701, hep-ph/2007.15656**
A. Berlin, R. T. D'Agnolo, **SARE,** K. Zhou

Decouples axion mass from detector volume

Heterodyne Resonator

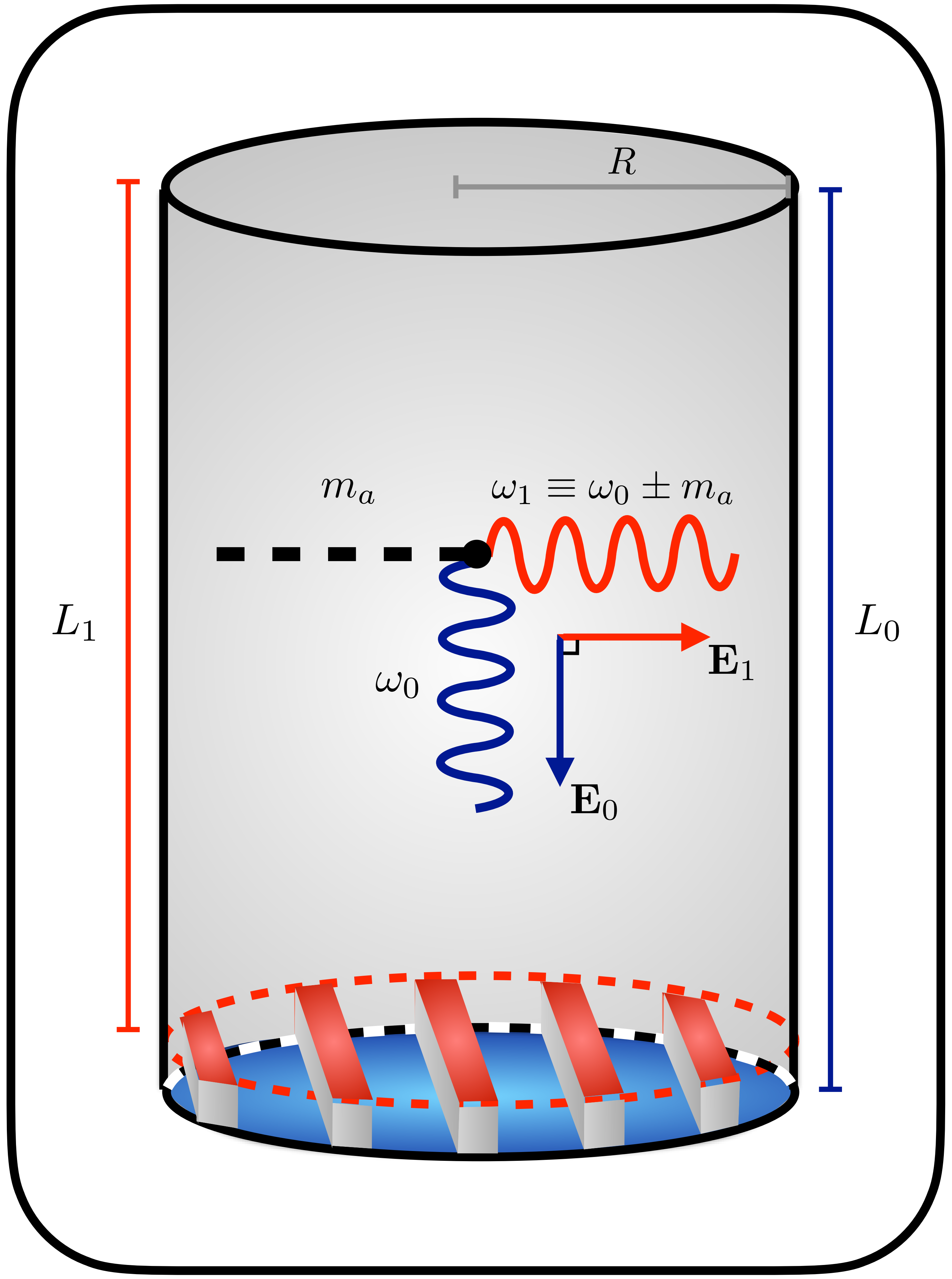

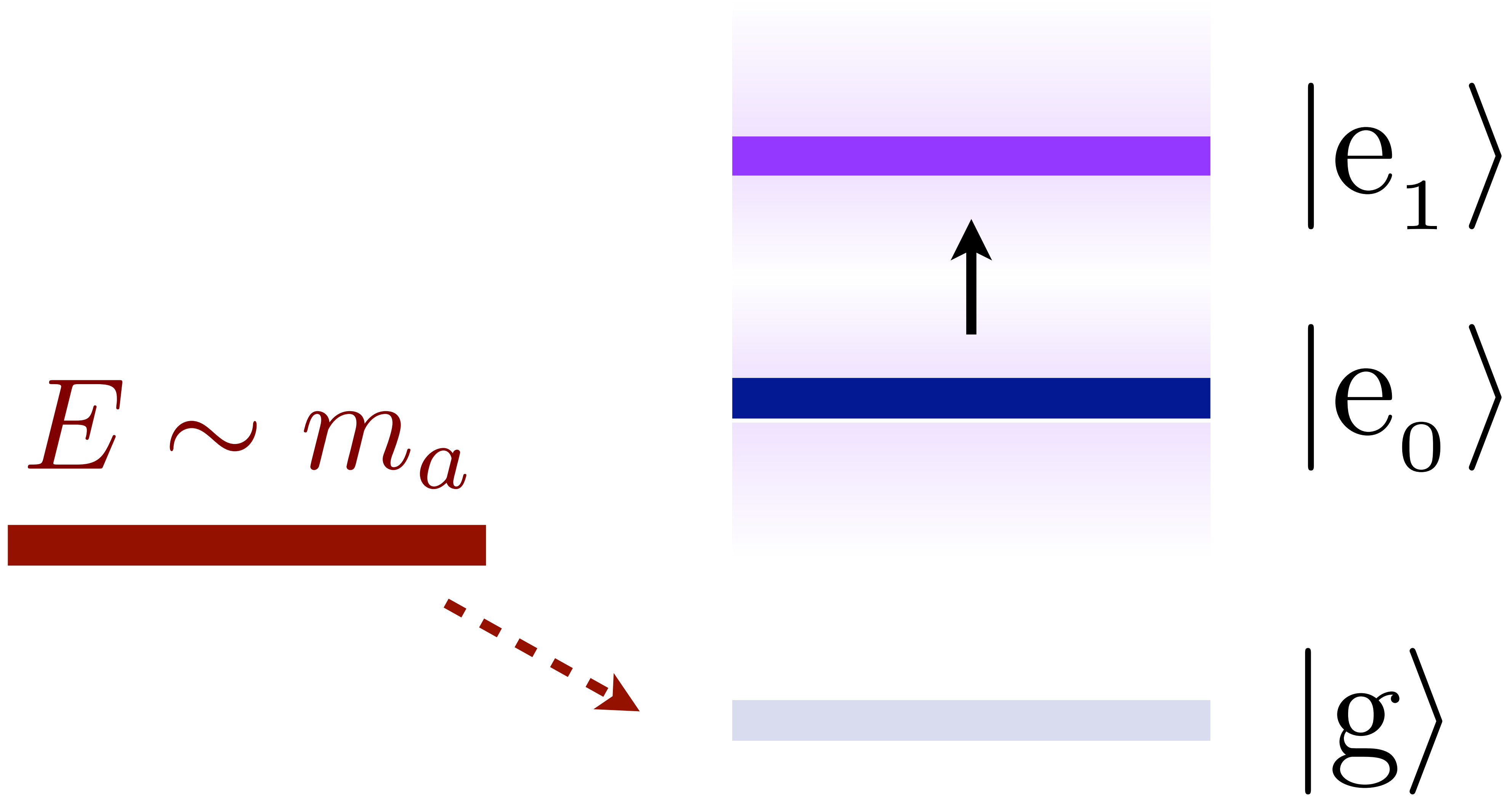

Ground state unpopulated

Heterodyne Resonator

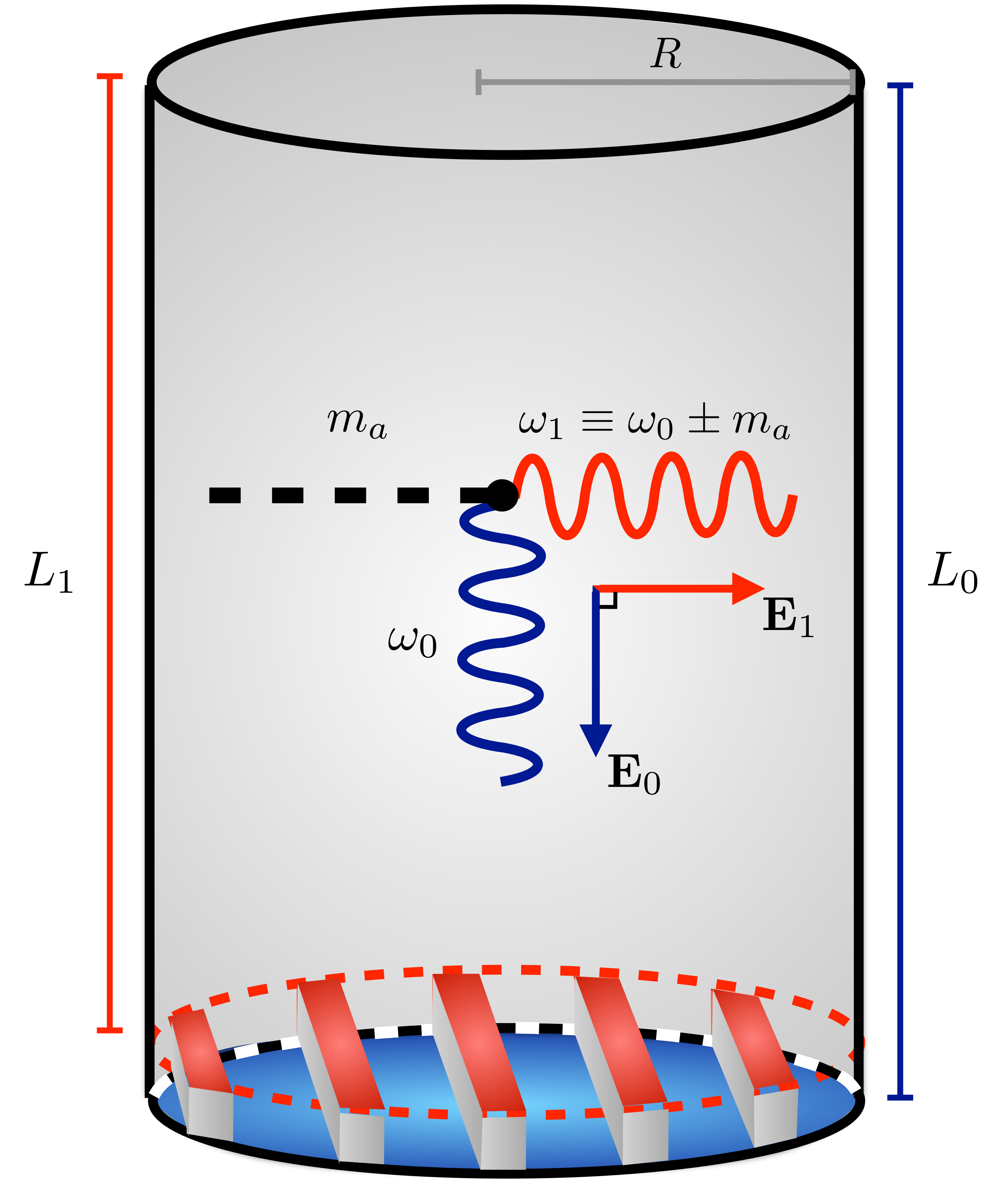

Geometry fixes splitting ΔE

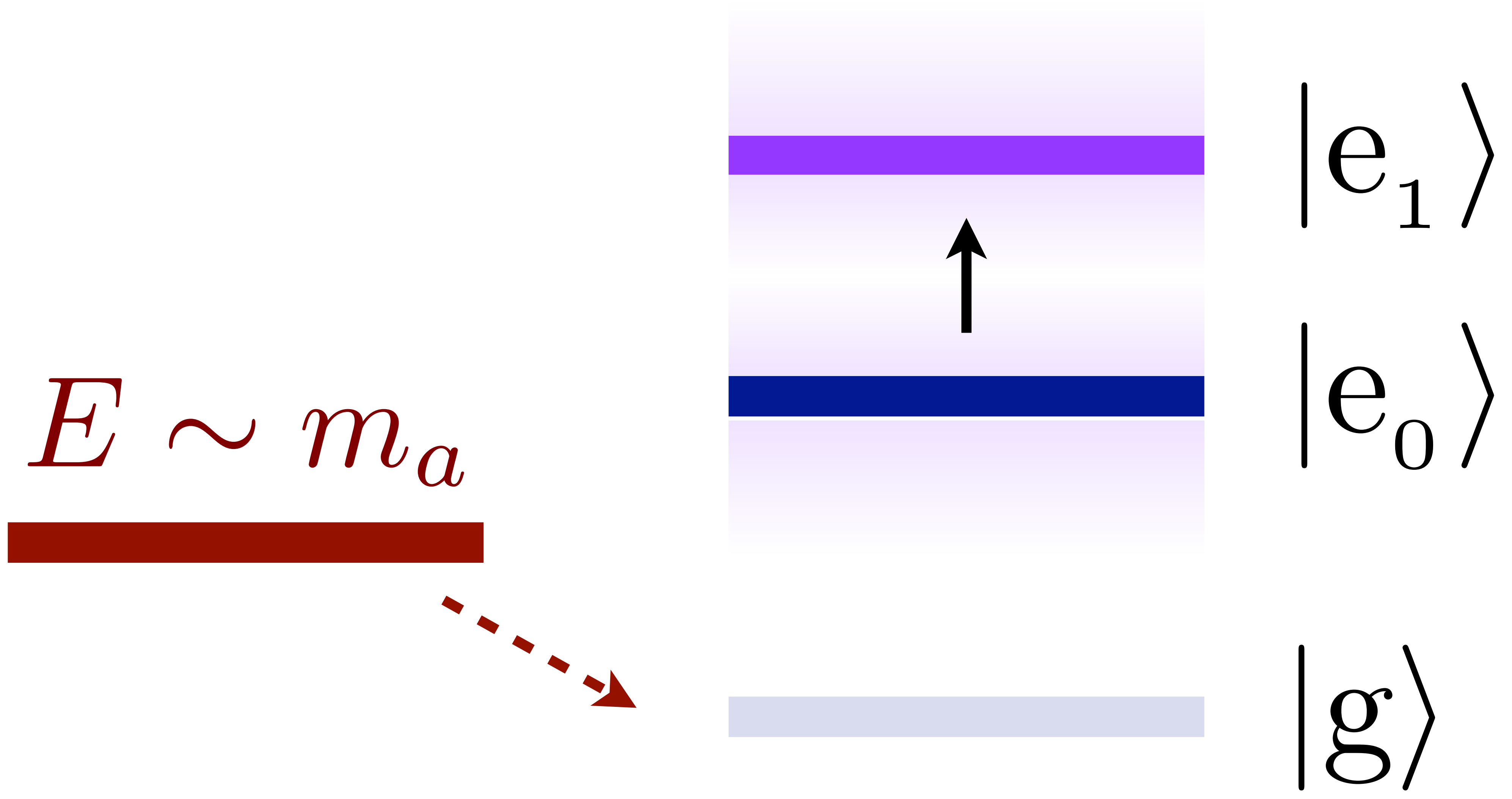

Ground state unpopulated

Tunability

$\delta\omega \ll \text{GHz}$

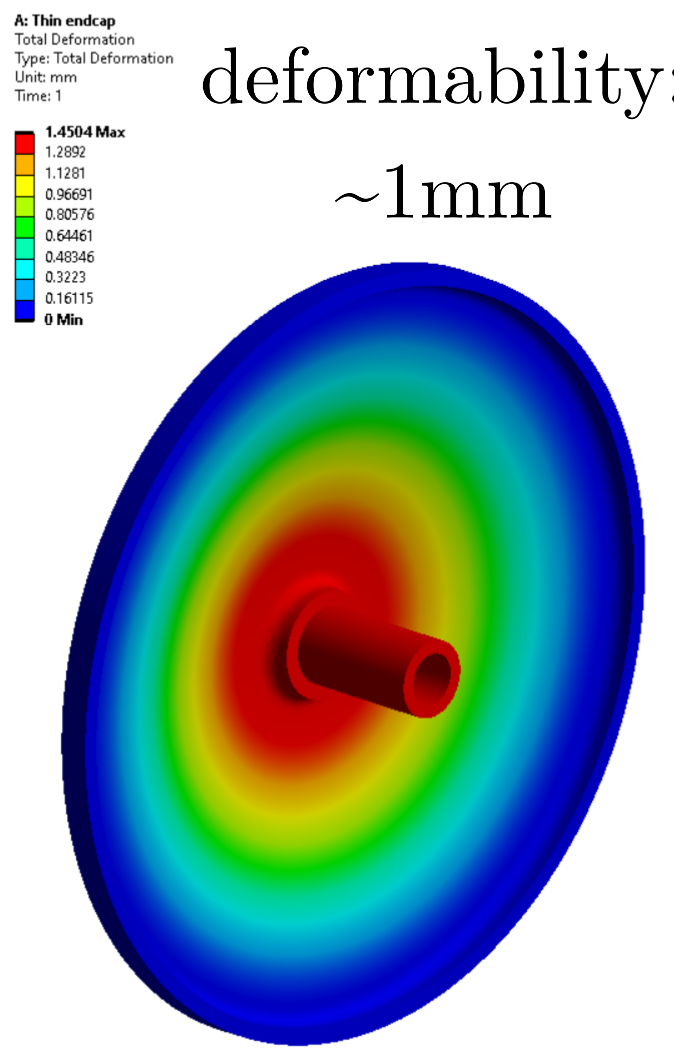

deformability:

~1mm

Courtesy: Marco Oriunno (SLAC)

Noise Sources

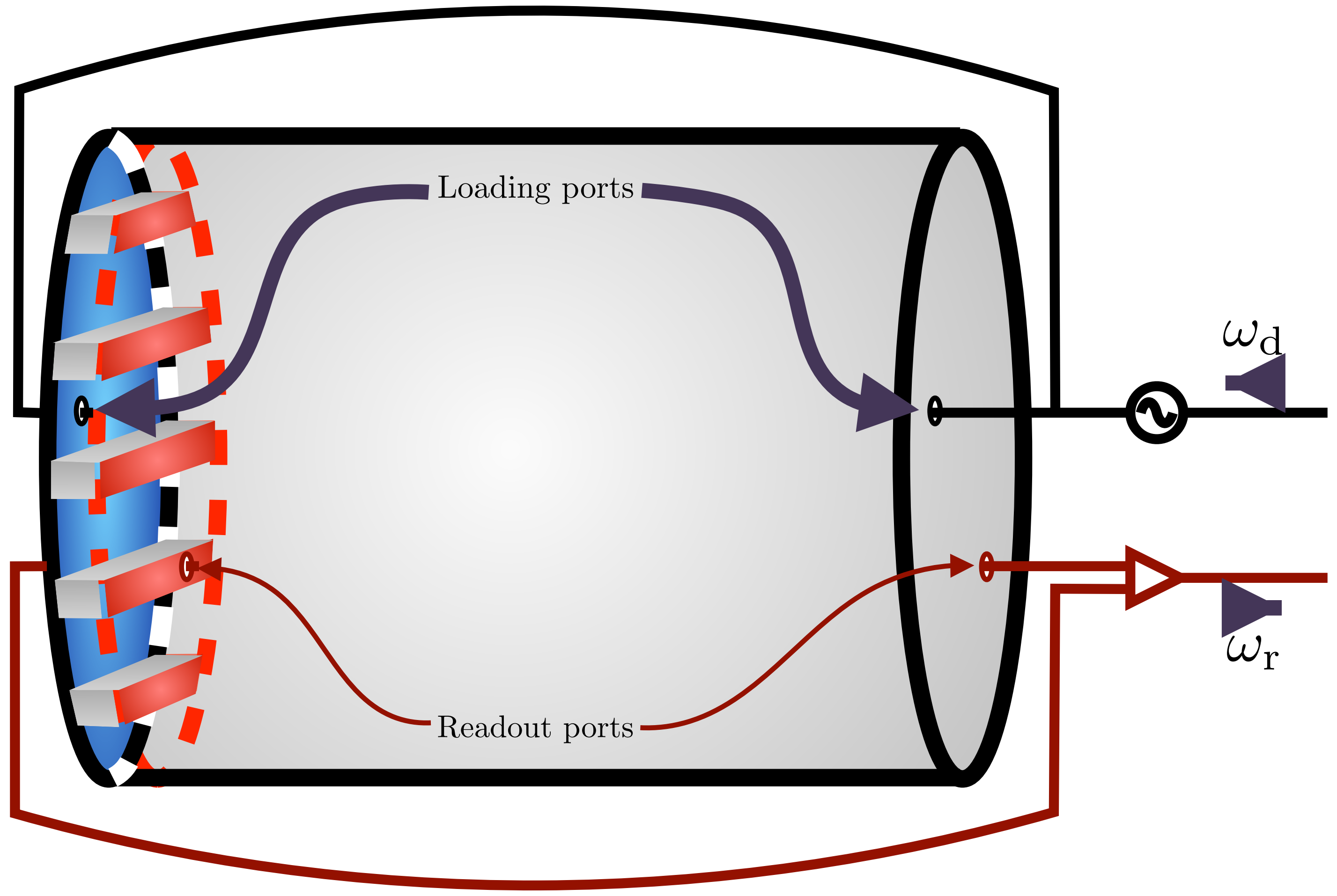

See backup for details on each noise source

Noise Sources

- ***Thermal noise***: requires cryo

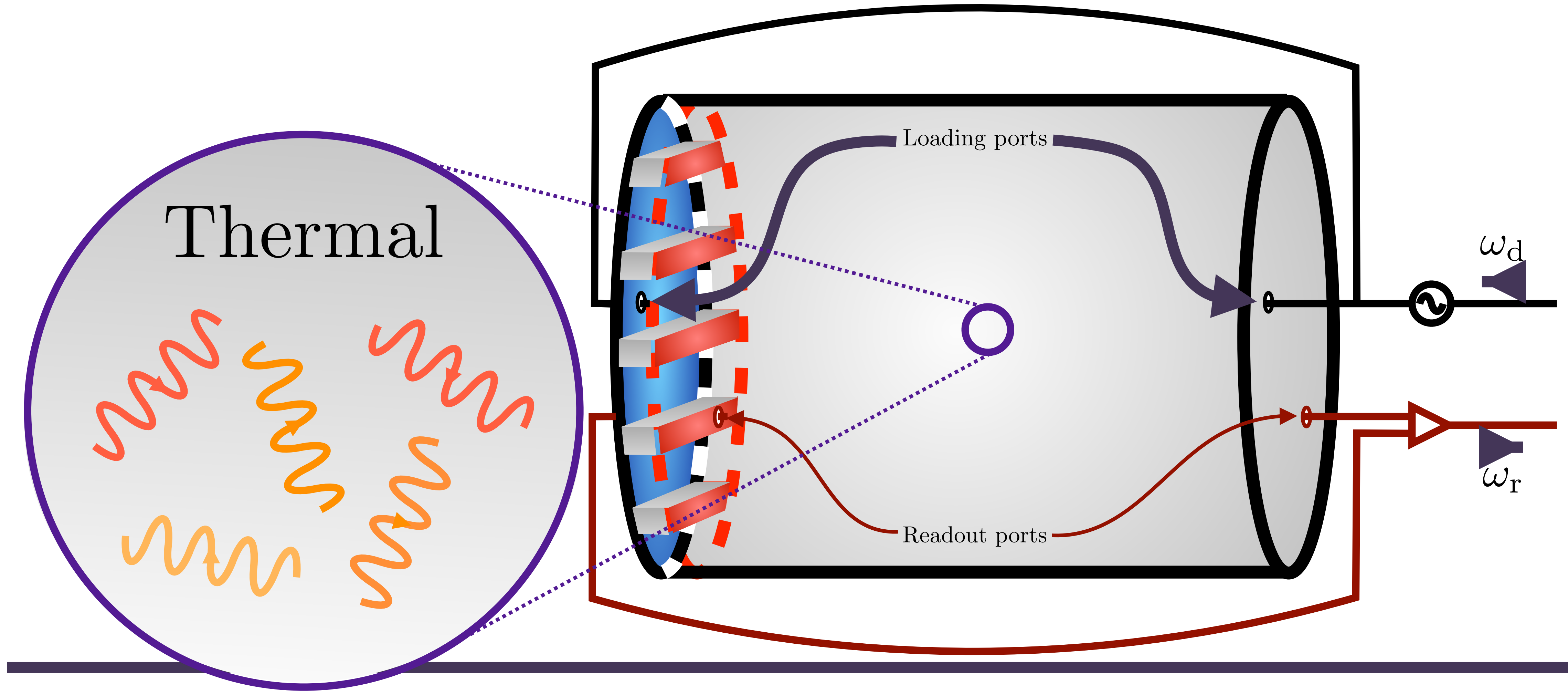

See backup for details on each noise source

Noise Sources

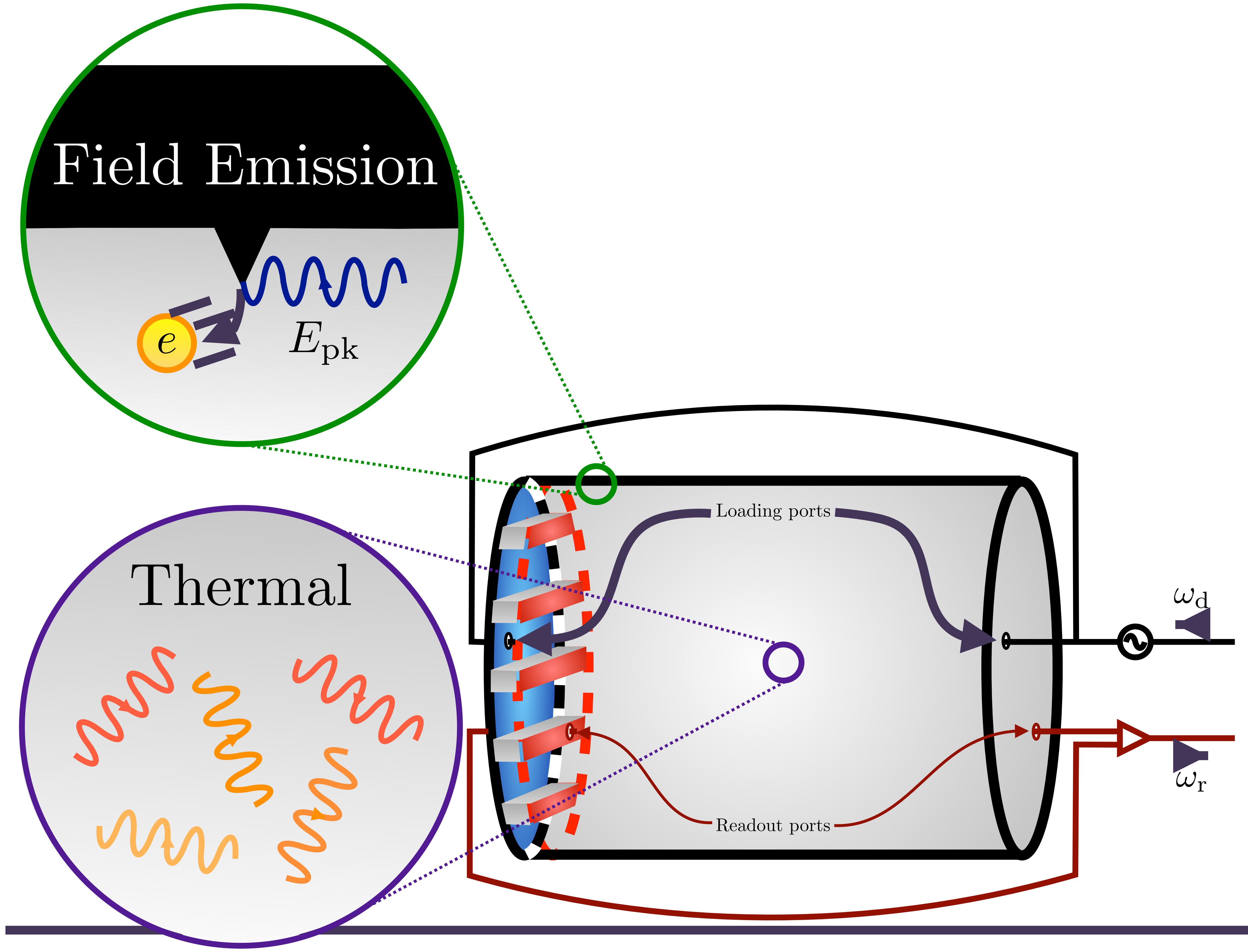

- ***Thermal noise***: requires cryo
- ***Field Emission***: careful design & limits peak B-field

See backup for details on each noise source

Noise Sources

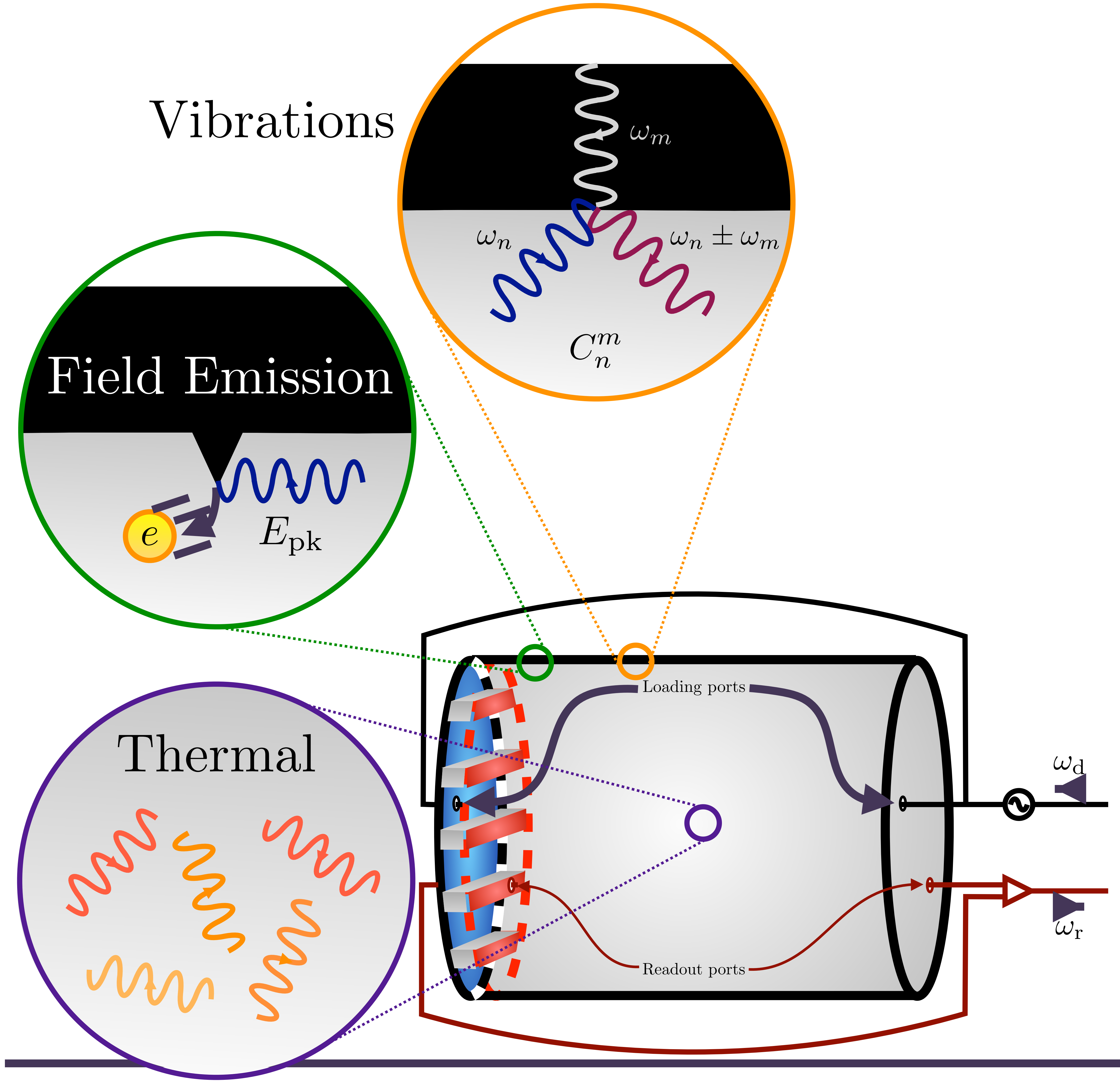

- ***Thermal noise***: requires cryo
- ***Field Emission***: careful design & limits peak B-field
- ***Vibrations***: design to reduce microphonics, isolation, cryo

See backup for details on each noise source

Noise Sources

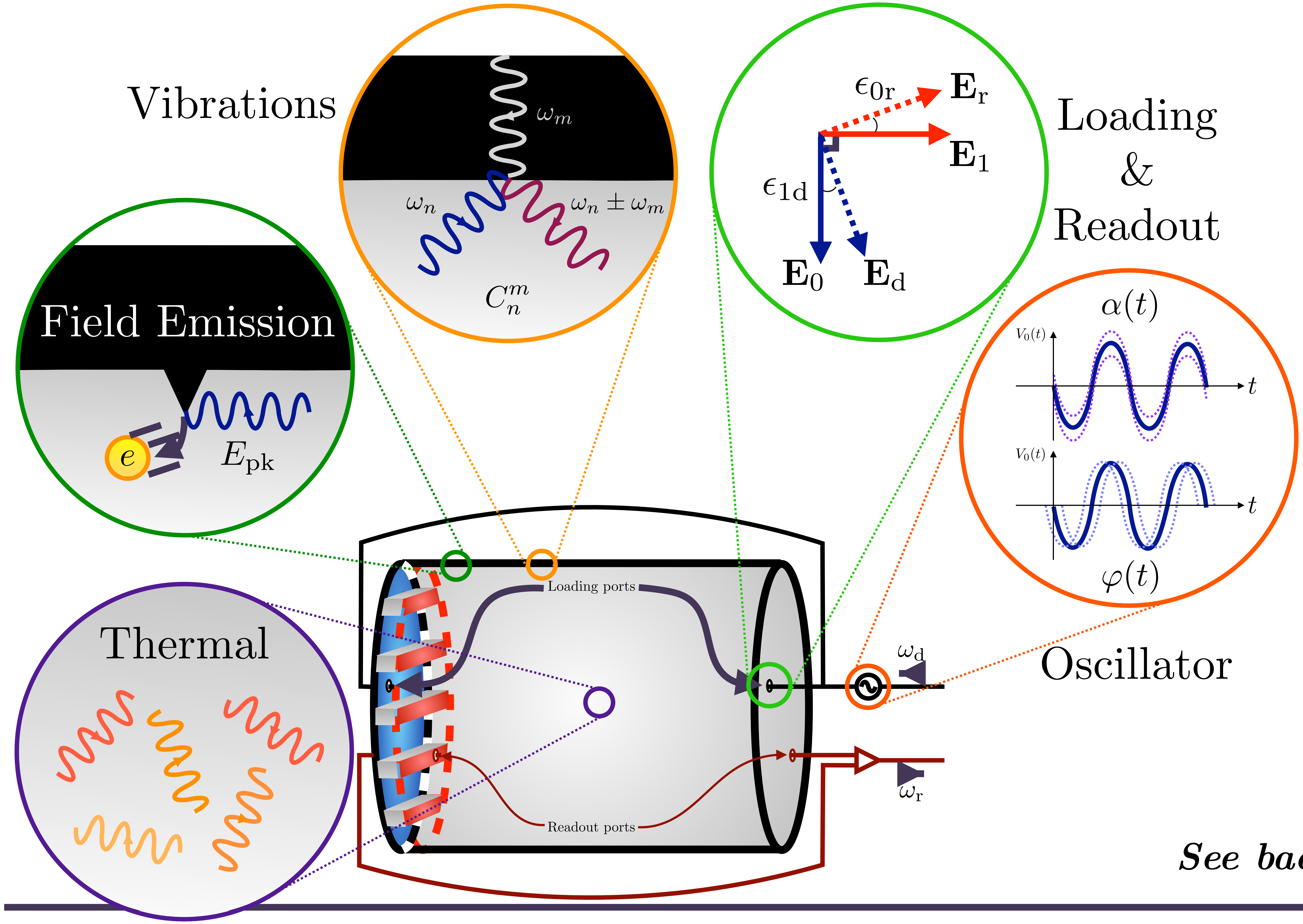

- ***Thermal noise***: requires cryo
- ***Field Emission***: careful design & limits peak B-field
- ***Vibrations***: design to reduce microphonics, isolation, cryo
- ***Loading/Readout & Phase***: design to improve coupling to pump & signal modes. Low phase-noise pump & readout electronics

See backup for details on each noise source

Cavity Response and Scanning

Cavity Response and Scanning

Overcoupling keeps SNR in bin constant but increases scan rate

Chaudhuri et al (2018)
Berlin et al (2019)

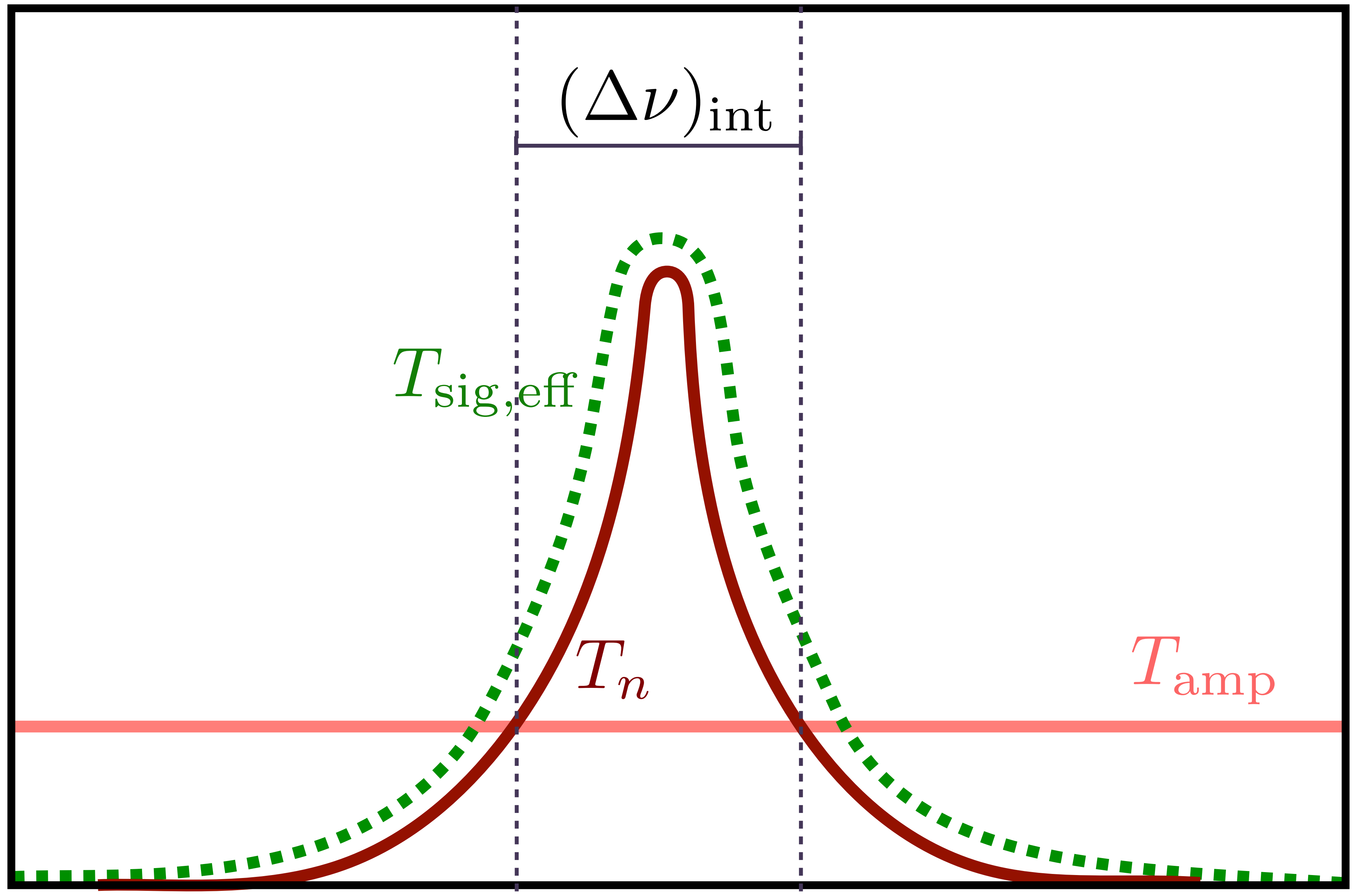

Cavity Response and Scanning

Overcoupling keeps SNR in bin constant but increases scan rate

Chaudhuri et al (2018)
Berlin et al (2019)

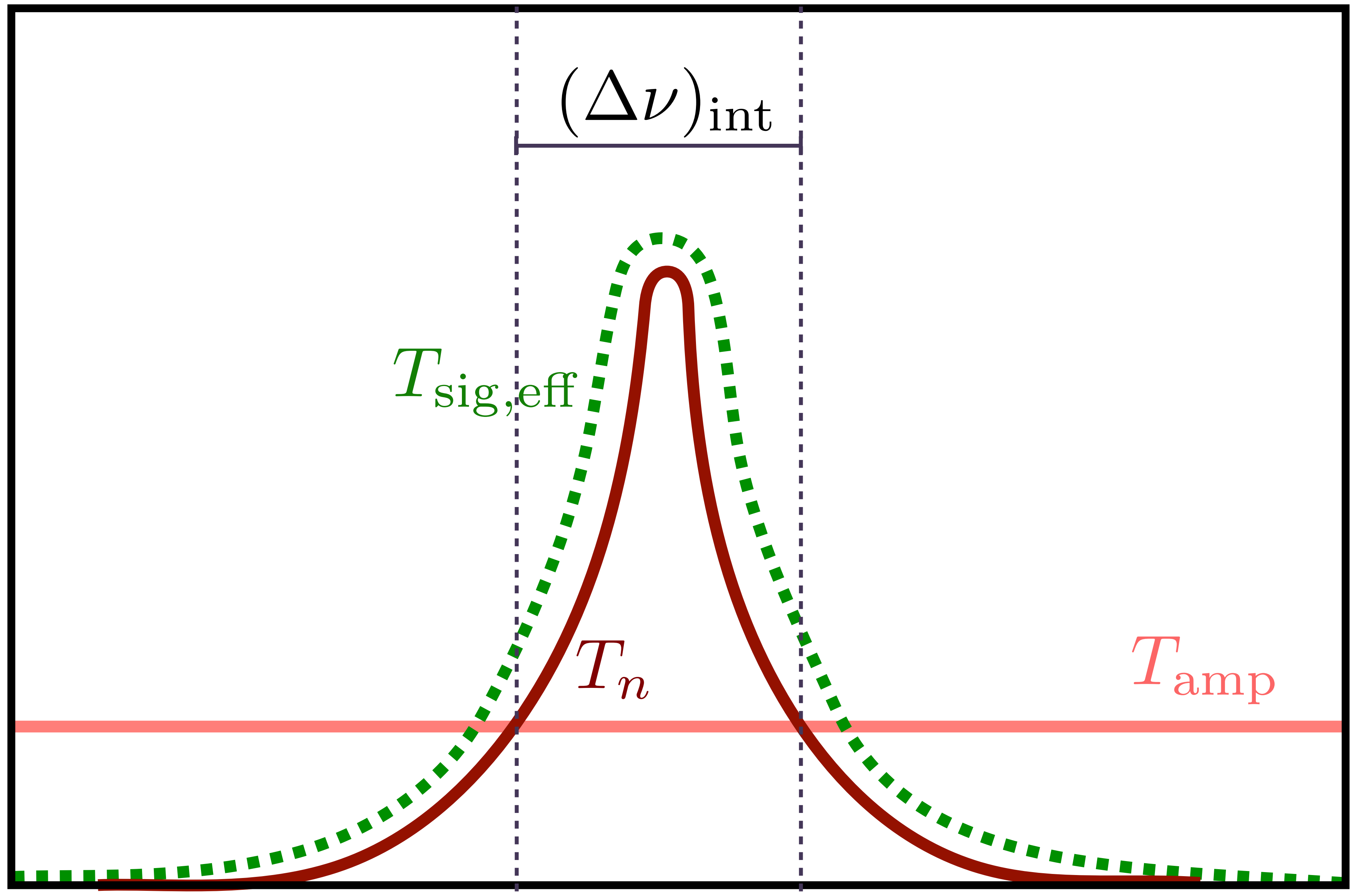

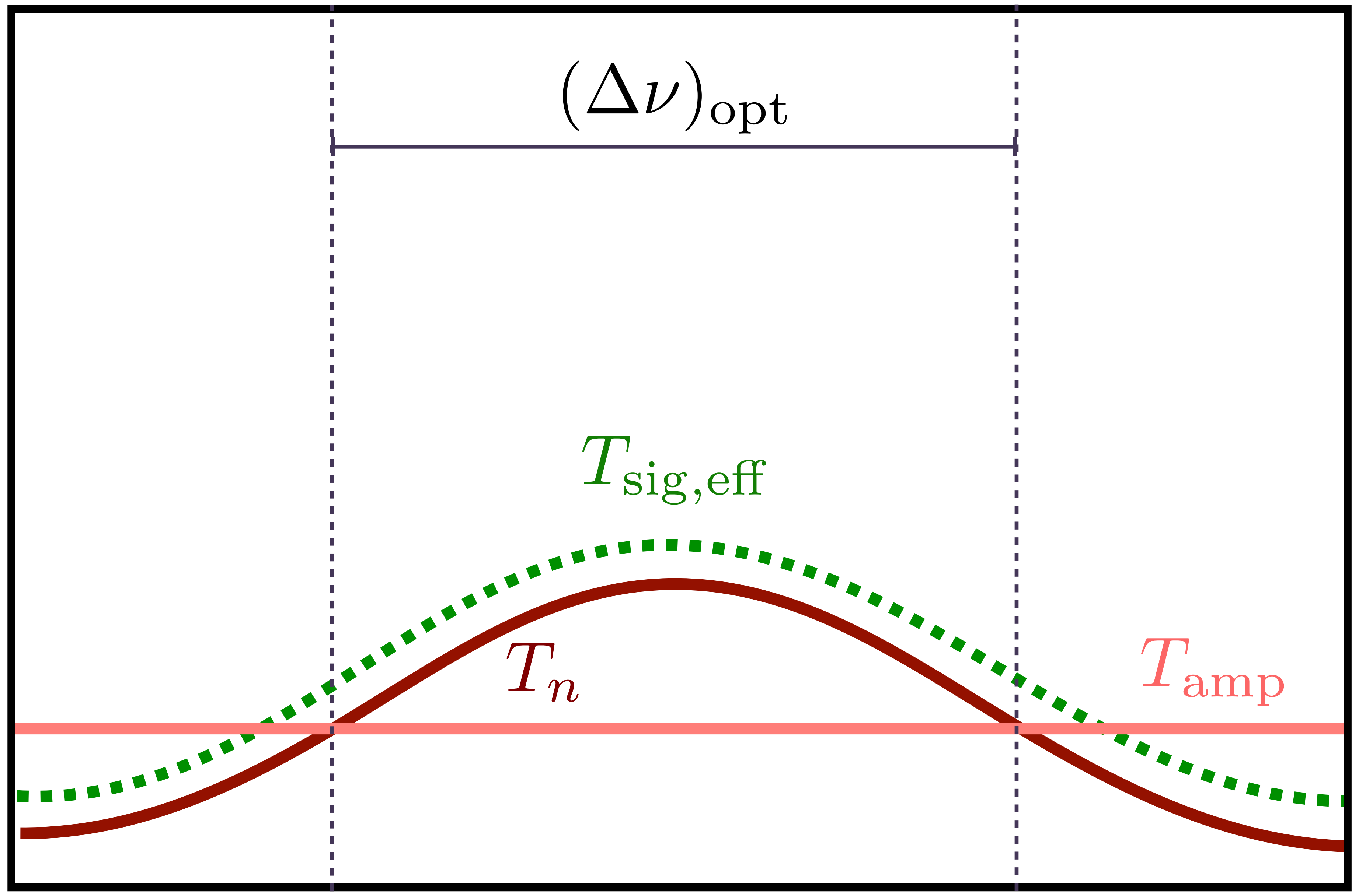

Cavity Response and Scanning

Overcoupling keeps SNR in bin constant but increases scan rate

Chaudhuri et al (2018)
Berlin et al (2019)

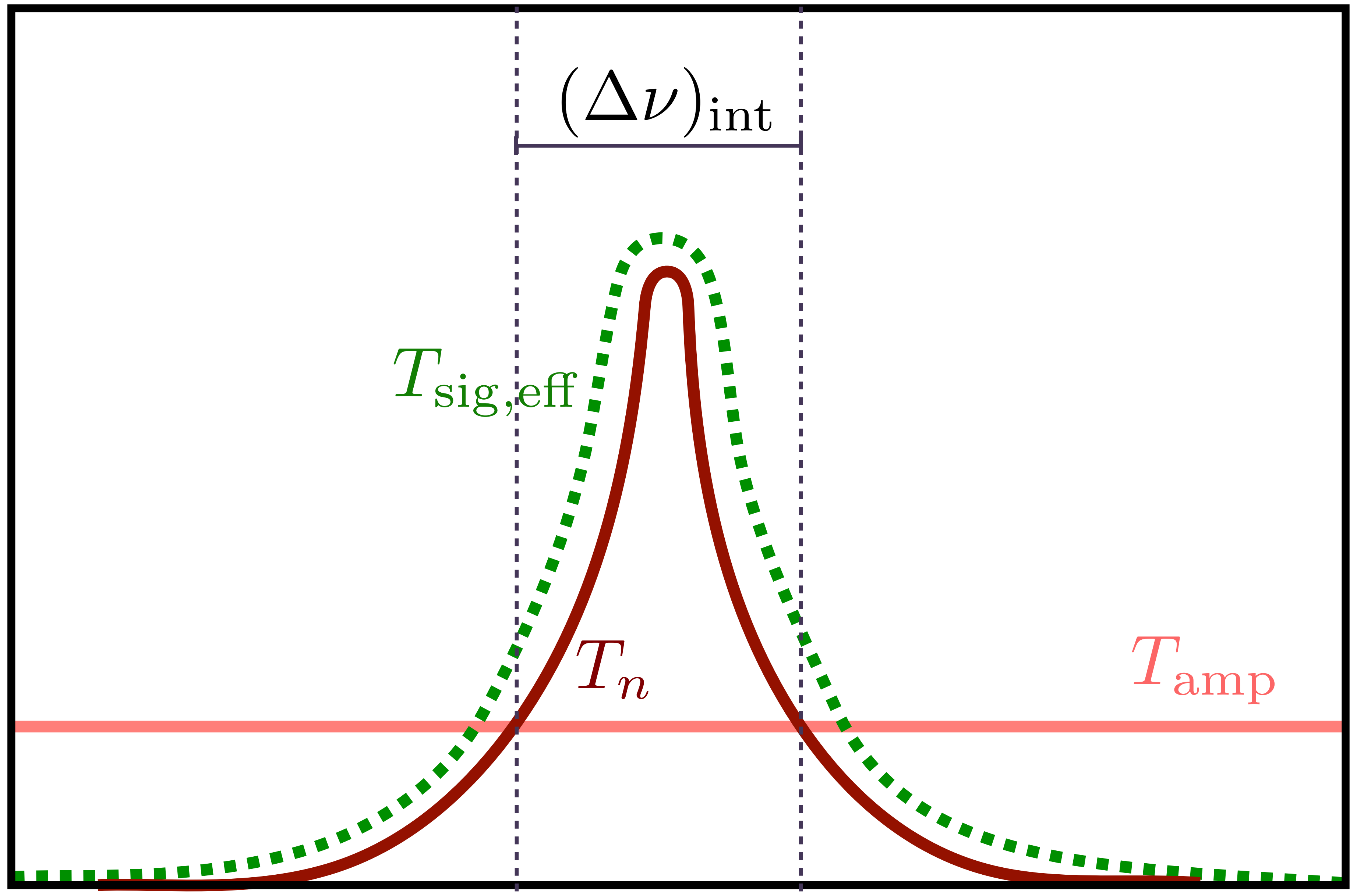

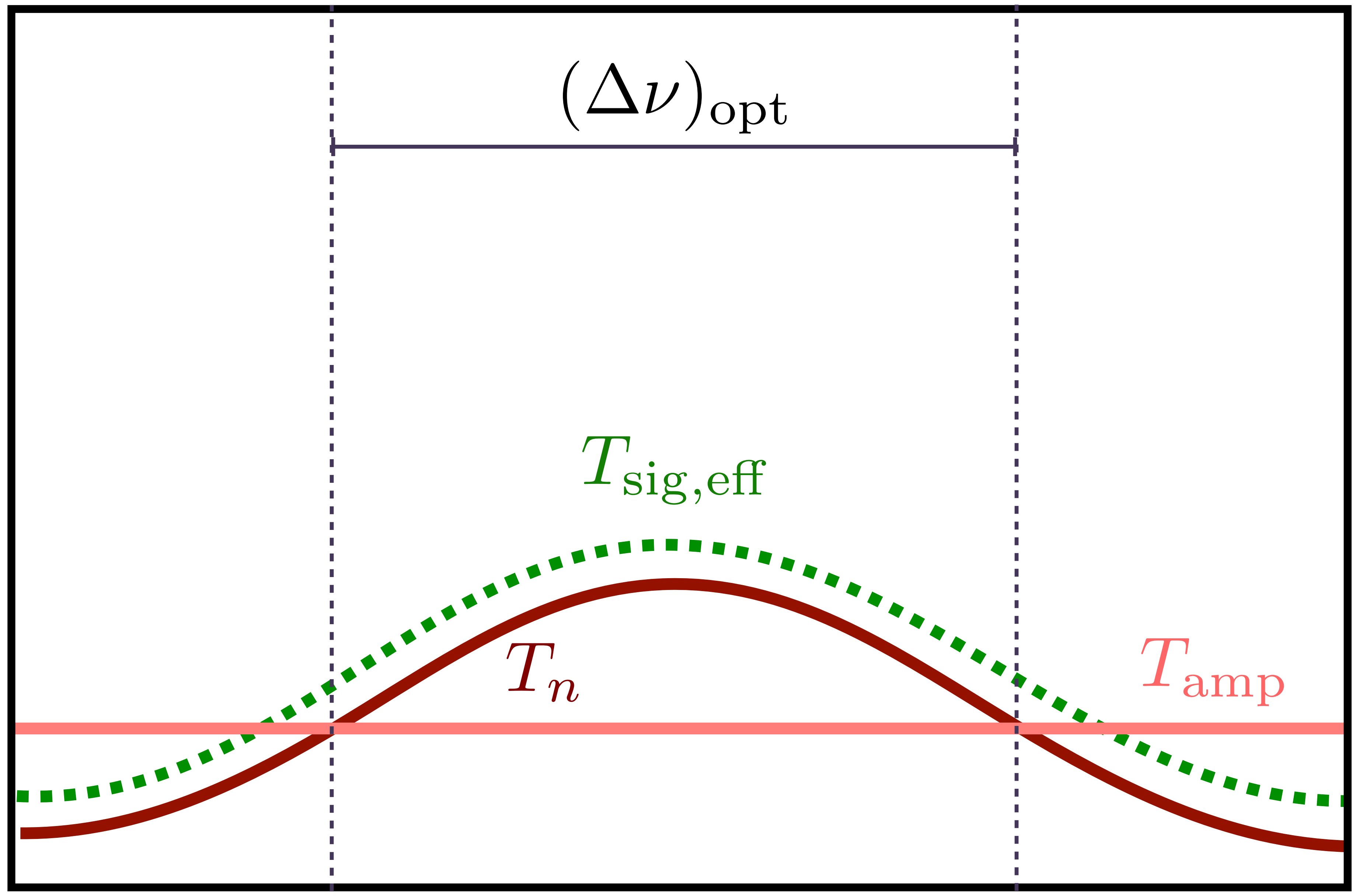

For SQL amplifier: $(\Delta\nu)_{\rm opt} \simeq n_{\rm occ}(\Delta\nu)_{\rm int}$

Cavity Response and Scanning

Overcoupling keeps SNR in bin constant but increases scan rate

Chaudhuri et al (2018)
Berlin et al (2019)

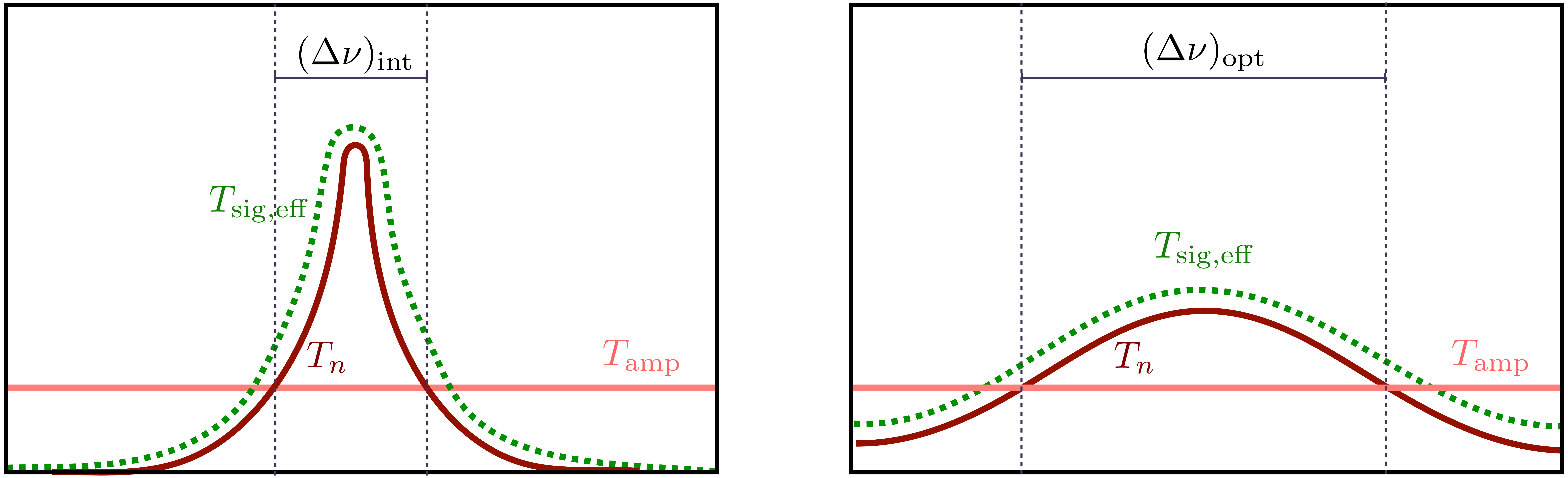

For SQL amplifier: $(\Delta\nu)_{\rm opt} \simeq n_{\rm occ}(\Delta\nu)_{\rm int}$

SRF: optimal $Q_L \sim Q_0/100$

Signal to Noise

Signal to Noise

Thermal noise dominated:

$$\mathrm{SNR} \sim \frac{\rho_{\mathrm{DM}}\, V}{m_a\, \omega_1} \left(g_{a\gamma\gamma}\, \eta_{10}\, B_0\right)^2 \left(\frac{Q_a\, Q_{\mathrm{int}}\, t_e}{T}\right)^{1/2}$$

Signal to Noise

Thermal noise dominated:

$$\mathrm{SNR} \sim \frac{\rho_{\mathrm{DM}}\, V}{m_a\, \omega_1} \left(g_{a\gamma\gamma}\, \eta_{10}\, B_0\right)^2 \left(\frac{Q_a\, Q_{\mathrm{int}}\, t_e}{T}\right)^{1/2}$$

Comparison with LC resonator:

$$\frac{\mathrm{SNR}}{\mathrm{SNR}^{\mathrm{LC}}} \sim \frac{\omega_0 \pm m_a}{m_a} \left(\frac{Q_{\mathrm{int}}}{Q_{\mathrm{LC}}}\right)^{1/2} \left(\frac{T_{\mathrm{LC}}}{T}\right)^{1/2} \left(\frac{B_0}{B_{\mathrm{LC}}}\right)^2$$

Signal to Noise

Thermal noise dominated:

$$\mathrm{SNR} \sim \frac{\rho_{\rm DM}\, V}{m_a\, \omega_1} \left(g_{a\gamma\gamma}\, \eta_{10}\, B_0\right)^2 \left(\frac{Q_a\, Q_{\rm int}\, t_e}{T}\right)^{1/2}$$

Comparison with LC resonator:

$$\frac{\mathrm{SNR}}{\mathrm{SNR}^{\rm LC}} \sim \frac{\omega_0 \pm m_a}{m_a} \left(\frac{Q_{\rm int}}{Q_{\rm LC}}\right)^{1/2} \left(\frac{T_{\rm LC}}{T}\right)^{1/2} \left(\frac{B_0}{B_{\rm LC}}\right)^2$$

Signal to Noise

Thermal noise dominated:

$$\mathrm{SNR} \sim \frac{\rho_{\mathrm{DM}}\, V}{m_a\, \omega_1} \left(g_{a\gamma\gamma}\, \eta_{10}\, B_0\right)^2 \left(\frac{Q_a\, Q_{\mathrm{int}}\, t_e}{T}\right)^{1/2}$$

Comparison with LC resonator:

$$\frac{\mathrm{SNR}}{\mathrm{SNR}^{\mathrm{LC}}} \sim \frac{\omega_0 \pm m_a}{m_a} \left(\frac{Q_{\mathrm{int}}}{Q_{\mathrm{LC}}}\right)^{1/2} \left(\frac{T_{\mathrm{LC}}}{T}\right)^{1/2} \left(\frac{B_0}{B_{\mathrm{LC}}}\right)^2$$

Signal to Noise

Thermal noise dominated:

$$\mathrm{SNR} \sim \frac{\rho_{\rm DM}\, V}{m_a\, \omega_1} \left(g_{a\gamma\gamma}\, \eta_{10}\, B_0\right)^2 \left(\frac{Q_a\, Q_{\rm int}\, t_e}{T}\right)^{1/2}$$

Comparison with LC resonator:

$$\frac{\mathrm{SNR}}{\mathrm{SNR}^{\rm LC}} \sim \frac{\omega_0 \pm m_a}{m_a} \left(\frac{Q_{\rm int}}{Q_{\rm LC}}\right)^{1/2} \left(\frac{T_{\rm LC}}{T}\right)^{1/2} \left(\frac{B_0}{B_{\rm LC}}\right)^2$$

Sensitivity

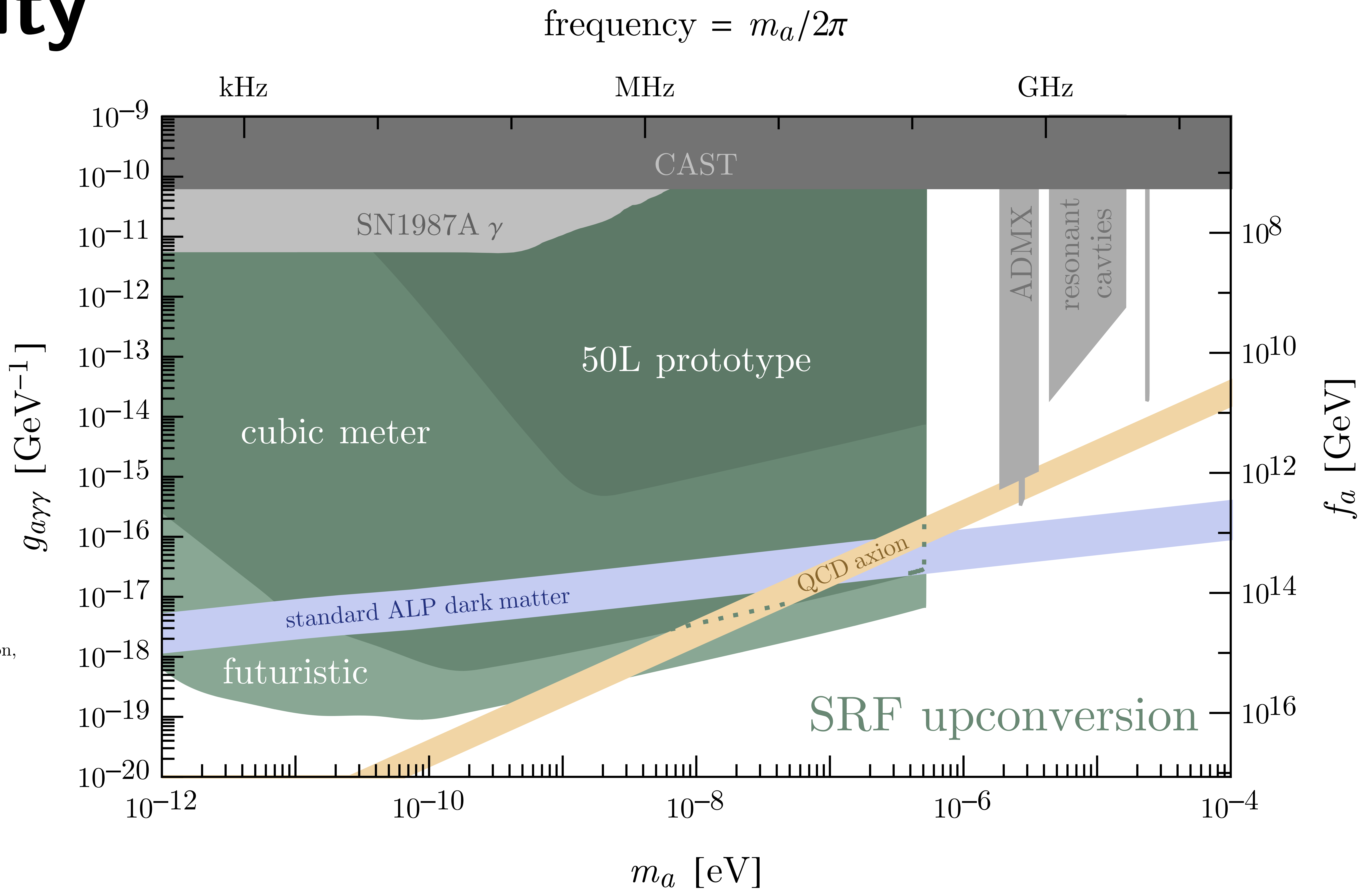

JHEP **07 (2020) 088, hep-ph/1912.11048**
A. Berlin, R. T. D'Agnolo, **SARE,** P. Schuster, N. Toro, C. Nantista, J. Neilson, S. Tantawi, K. Zhou

PRD **104 (2021) 11, L111701, hep-ph/2007.15656**
A. Berlin, R. T. D'Agnolo, **SARE,** K. Zhou

Sensitivity

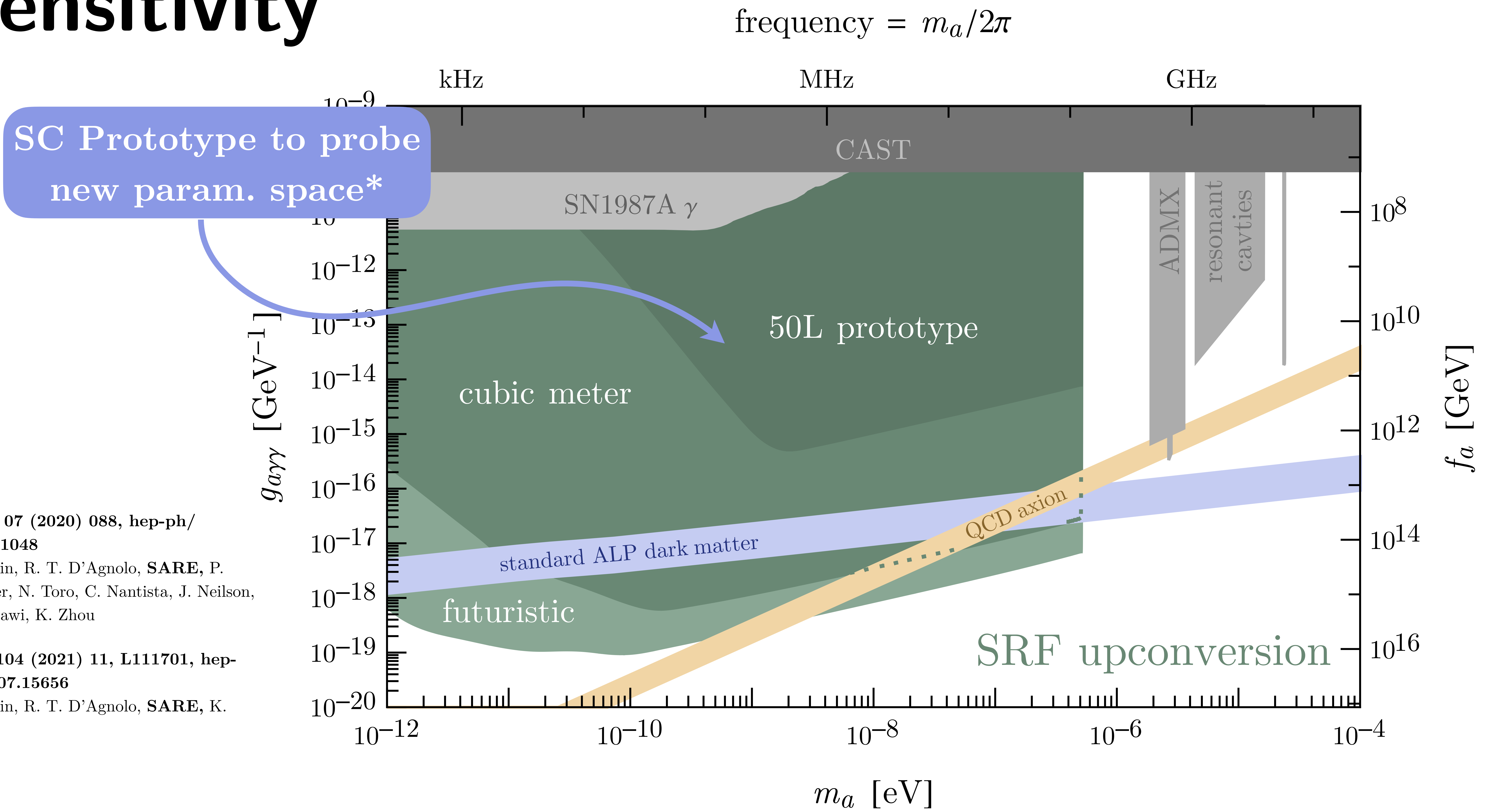

JHEP **07 (2020) 088, hep-ph/1912.11048**
A. Berlin, R. T. D'Agnolo, **SARE,** P. Schuster, N. Toro, C. Nantista, J. Neilson, S. Tantawi, K. Zhou

PRD **104 (2021) 11, L111701, hep-ph/2007.15656**
A. Berlin, R. T. D'Agnolo, **SARE,** K. Zhou

Sensitivity

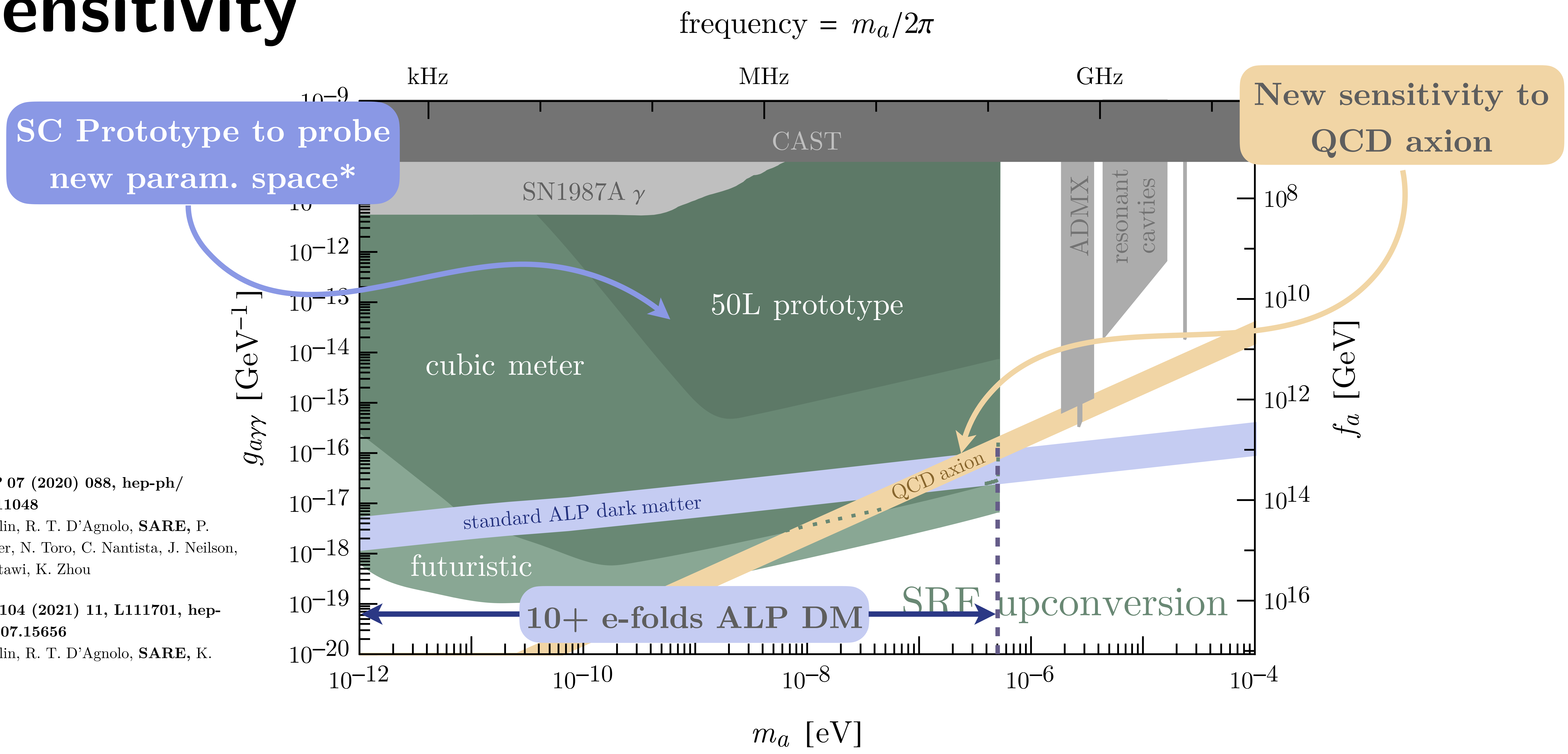

***JHEP* 07 (2020) 088, hep-ph/ 1912.11048**
A. Berlin, R. T. D'Agnolo, **SARE,** P. Schuster, N. Toro, C. Nantista, J. Neilson, S. Tantawi, K. Zhou

***PRD* 104 (2021) 11, L111701, hep-ph/2007.15656**
A. Berlin, R. T. D'Agnolo, **SARE,** K. Zhou

Current Status

SLAC

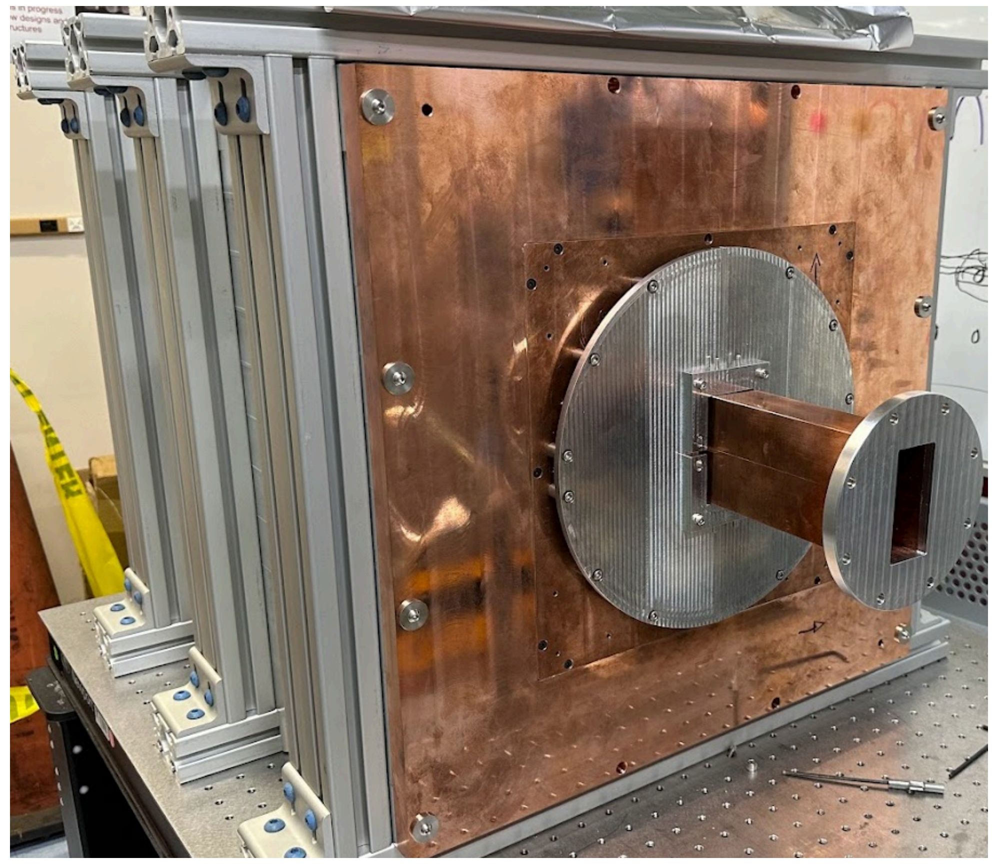

LDRD led by S. Tantawi

- Copper prototype
- Input from PBC
- Data-taking ongoing

CERN

CERN | Physics Beyond Colliders

QUANTUM TECHNOLOGY INITIATIVE

- PBC since ~2021
- QTI since Jan. 2024

FNAL

Giaccone et al [hep-ex/2207.11346]

- Single-cell SRF
- Cavity prep ongoing

Summary

Heterodyne approach achieves parametric gain for small axion masses vs. static searches

$$\frac{\mathrm{SNR}}{\mathrm{SNR}^{\mathrm{LC}}} \sim \frac{\omega_0 \pm m_a}{m_a}\left(\frac{Q_{\mathrm{int}}}{Q_{\mathrm{LC}}}\right)^{1/2}\left(\frac{T_{\mathrm{LC}}}{T}\right)^{1/2}\left(\frac{B_0}{B_{\mathrm{LC}}}\right)^{2}$$

Technology Requirements:

- **High overlap between pumped cavity mode and signal mode**
- **Low phase noise power source**
- **Low microphonics**
- **High-precision machining of cavity to minimise deformation-induced mode-mixing**
- **Axion search technology could be used for a Gravitational Wave search** — *possibly in same cavity?*

BACKUP

Comparison of approaches

	Static-field Haloscope	LC Resonator	RF Frequency Conversion
J_{eff}	$\propto B_0^{\text{static}} \cos(m_a t)$	$\propto B_0^{\text{static}} \cos(m_a t)$	$\propto B_0^{\text{RF}} \cos(\omega_0 \pm m_a)t$
$\mathcal{E}_a$	$\propto m_a/\omega_{\text{sig}} \sim 1$	$\propto m_a V^{1/3} \lesssim 1$	$\propto (\omega_0 \pm m_a)/\omega_{\text{sig}} \sim 1$
P_{sig}	$J_{\text{eff}}^2 V \min\left(\frac{Q_{\text{r}}}{m_a}, \frac{Q_a}{m_a}\right)$	$J_{\text{eff}}^2 m_a^2 V^{5/3} \min\left(\frac{Q_{\text{LC}}}{m_a}, \frac{Q_a}{m_a}\right)$	$J_{\text{eff}}^2 V \min\left(\frac{Q_{\text{SRF}}}{\omega_0 \pm m_a}, \frac{Q_a}{m_a}\right)$

Axion Signal

Signal Power Spectral Density (PSD):

$$S_{\rm sig}(\omega) = \frac{\omega_1}{Q_1}\,(g_{a\gamma\gamma}\,\eta_{10}\,B_0)^2\,V\,\frac{\omega^2}{(\omega^2-\omega_1^2)^2+(\omega\,\omega_1/Q_1)^2}\int\frac{d\omega'}{(2\pi)^2}\,(\omega'-\omega)^2\,S_{b_0}(\omega')\,S_a(\omega-\omega')$$

Axion PSD: $\langle a(t)^2\rangle = \frac{1}{(2\pi)^2}\int d\omega\;S_a(\omega) = \frac{\rho_{\rm DM}}{m_a^2}$

Background magnetic field PSD:

$$S_{b_i}(\omega) = \pi^2\Big(\delta(\omega-\omega_i)+\delta(\omega+\omega_i)\Big) + S_{b_i}^{(\rm phase)} + S_{b_i}^{(\rm mech)}$$

NB: $B_i \equiv \sqrt{\frac{1}{V_{\rm cav}}\int_{V_{\rm cav}}|\mathbf{B}_i(x)|^2}$ $\qquad \mathbf{B}_i(x,t) = \mathbf{B}_i(x)\,b_i(t)$

Axion Signal

Signal Power Spectral Density (PSD):

$$S_{\rm sig}(\omega) = \frac{\omega_1}{Q_1} \left(g_{a\gamma\gamma}\, \eta_{10}\, B_0\right)^2 V \, \frac{\omega^2}{(\omega^2 - \omega_1^2)^2 + (\omega\, \omega_1/Q_1)^2} \int \frac{d\omega'}{(2\pi)^2} \, (\omega' - \omega)^2 \, S_{b_0}(\omega')\, S_a(\omega - \omega')$$

Signal Power (resonant):

$$P_{\rm sig} \simeq \frac{1}{4} \left(g_{a\gamma\gamma}\, \eta_{10}\, B_0\right)^2 \, \rho_{\rm DM} \, V \times \begin{cases} Q_1/\omega_1 & \frac{m_a}{Q_a} \ll \frac{\omega_1}{Q_1} \\ \pi Q_a/m_a & \frac{m_a}{Q_a} \gg \frac{\omega_1}{Q_1} \end{cases} ,$$

Standard Noise Sources: Thermal Noise

Power Spectral Density:

$$S_{\rm th}(\omega) = \frac{Q_1}{Q_{\rm int}} \frac{4\pi T\,(\omega\,\omega_1/Q_1)^2}{(\omega^2-\omega_1^2)^2+(\omega\,\omega_1/Q_1)^2}$$

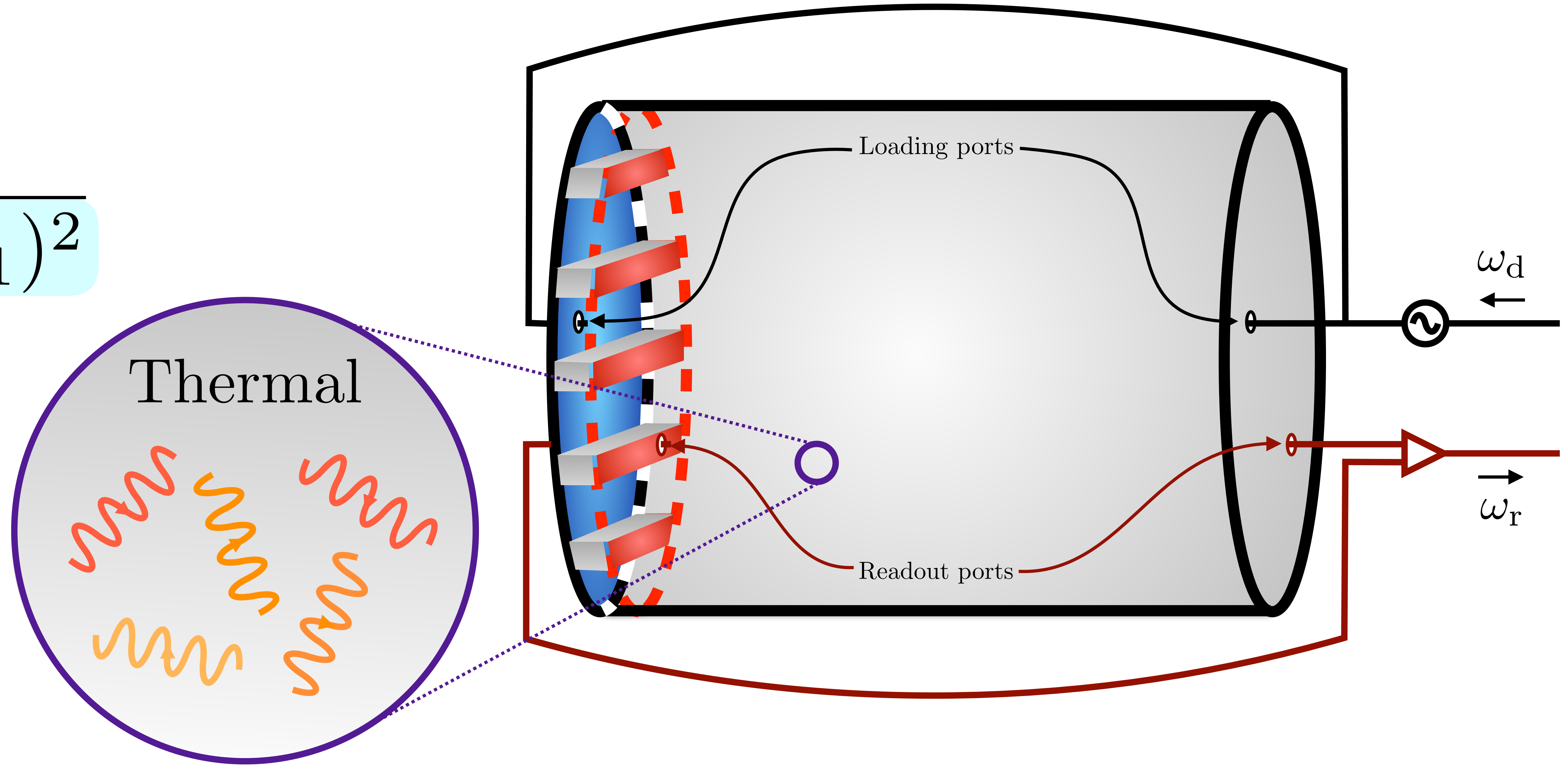

Non-standard Noise Sources: Phase Noise

Power Spectral Density:

$$S_{\text{phase}}(\omega) \simeq \frac{1}{2}\,\epsilon_{1\text{d}}^2\, S_\varphi(\omega - \omega_0)$$
$$\times \frac{(\omega\,\omega_1/Q_1)^2}{(\omega^2 - \omega_1^2)^2 + (\omega\,\omega_1/Q_1)^2}\,\frac{\omega_0 Q_1}{\omega_1 Q_0}\,P_{\text{in}}$$

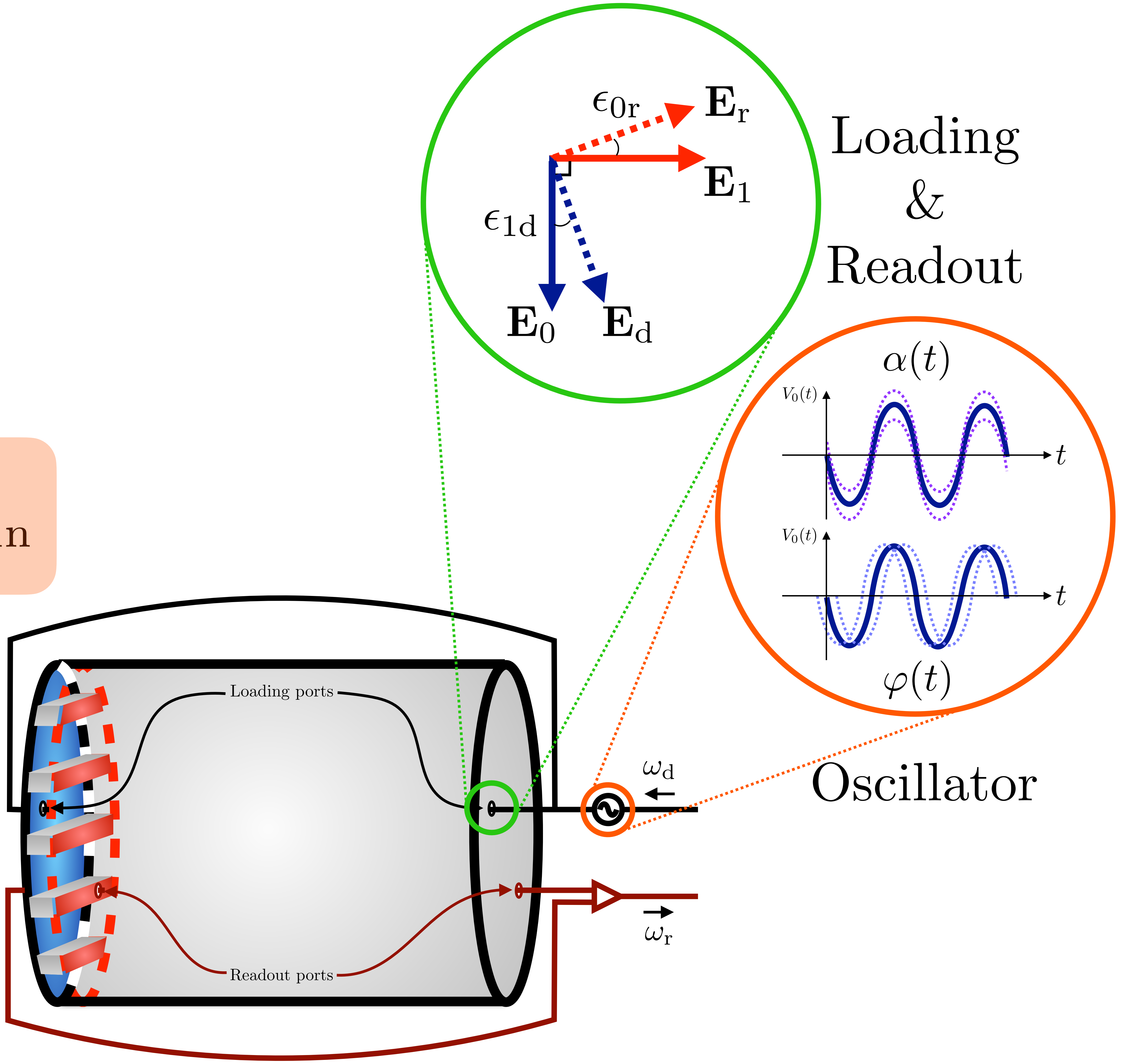

Non-standard Noise Sources: Vibrations

Vibrations

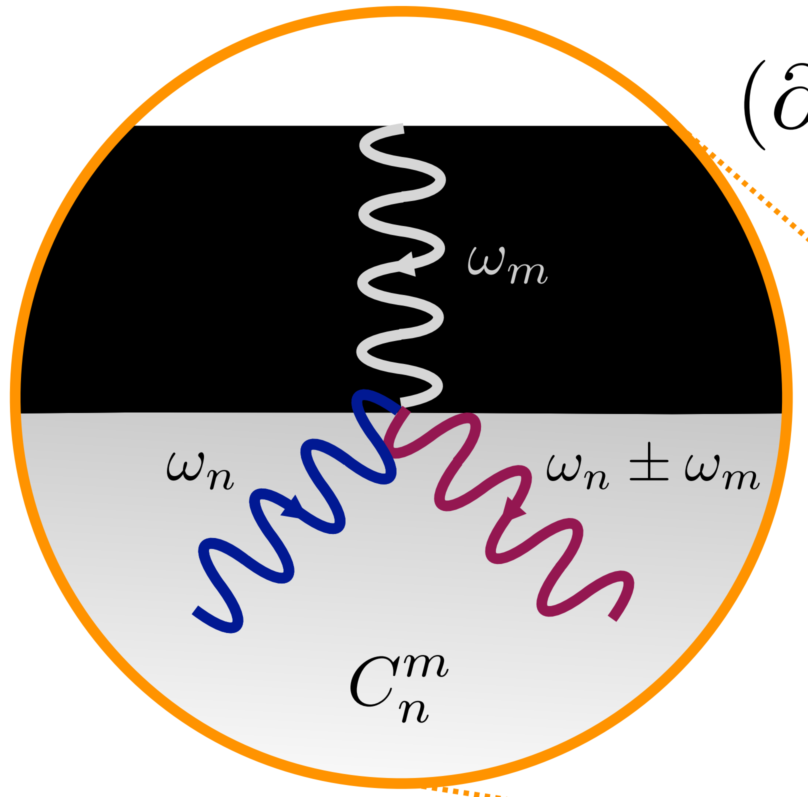

$$(\partial_t^2 + \omega_n^2)\, e_n \simeq \frac{2}{U_n} \sum_m e_m \begin{cases} \int_{\Delta V} d^3\mathbf{x} \left[\omega_n\, \omega_m\, \mathbf{B}_m \cdot \mathbf{B}_n^* - \frac{1}{2}\,(\omega_n^2 + \omega_m^2)\, \mathbf{E}_m \cdot \mathbf{E}_n^*\right] + \mathcal{O}(\Delta V^2) & (V' \subset V) \\ \int_{\Delta V} d^3\mathbf{x} \left[\omega_n\, \omega_m\, \mathbf{B}_m \cdot \mathbf{B}_n^* - \omega_n^2\, \mathbf{E}_m \cdot \mathbf{E}_n^*\right] + \mathcal{O}(\Delta V^2) & (V \subset V') \end{cases}$$

Cavity perturbation theory, see e.g. Meidlinger (2009), Pozar, etc.

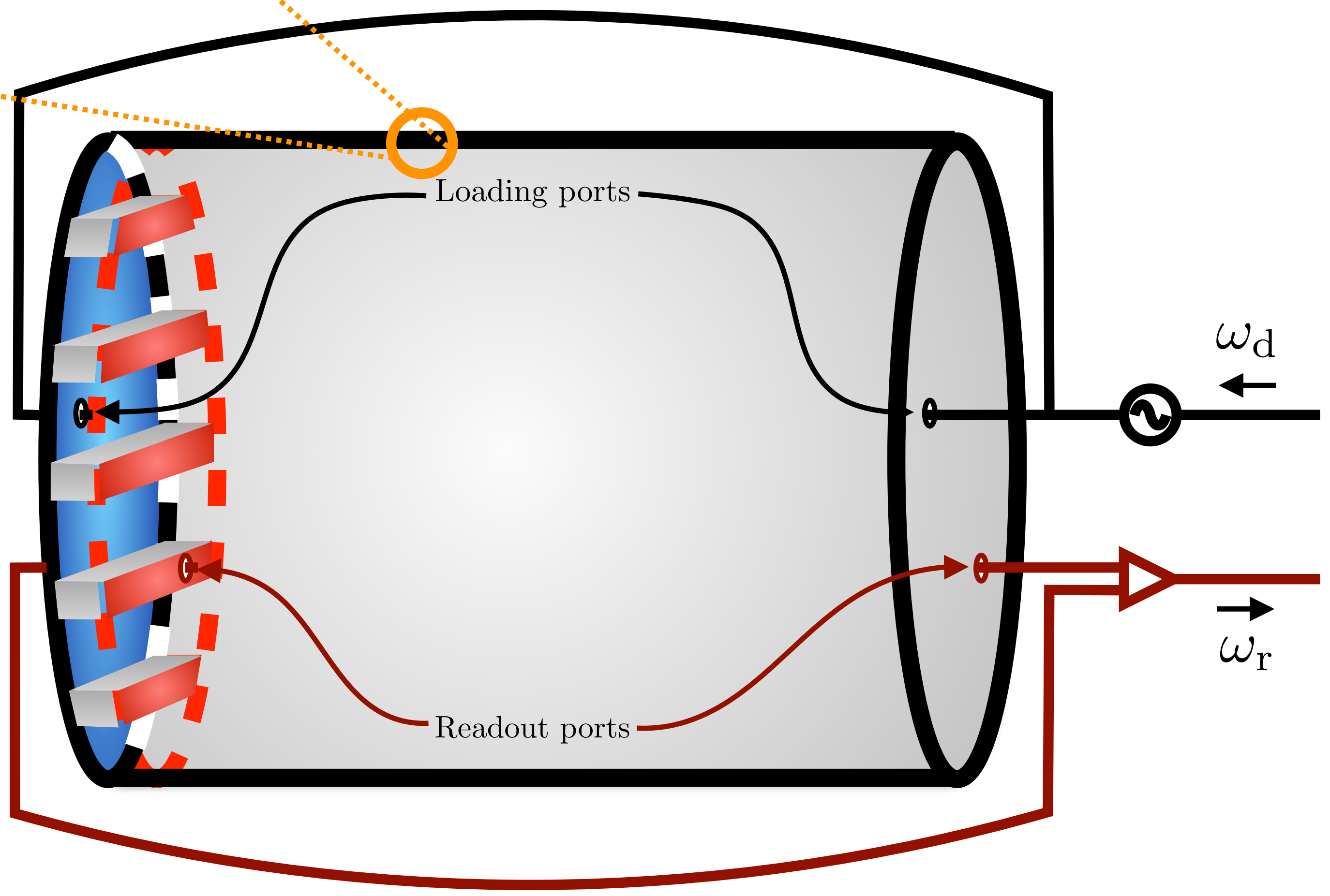

Non-standard Noise Sources: Vibrations

Vibrations

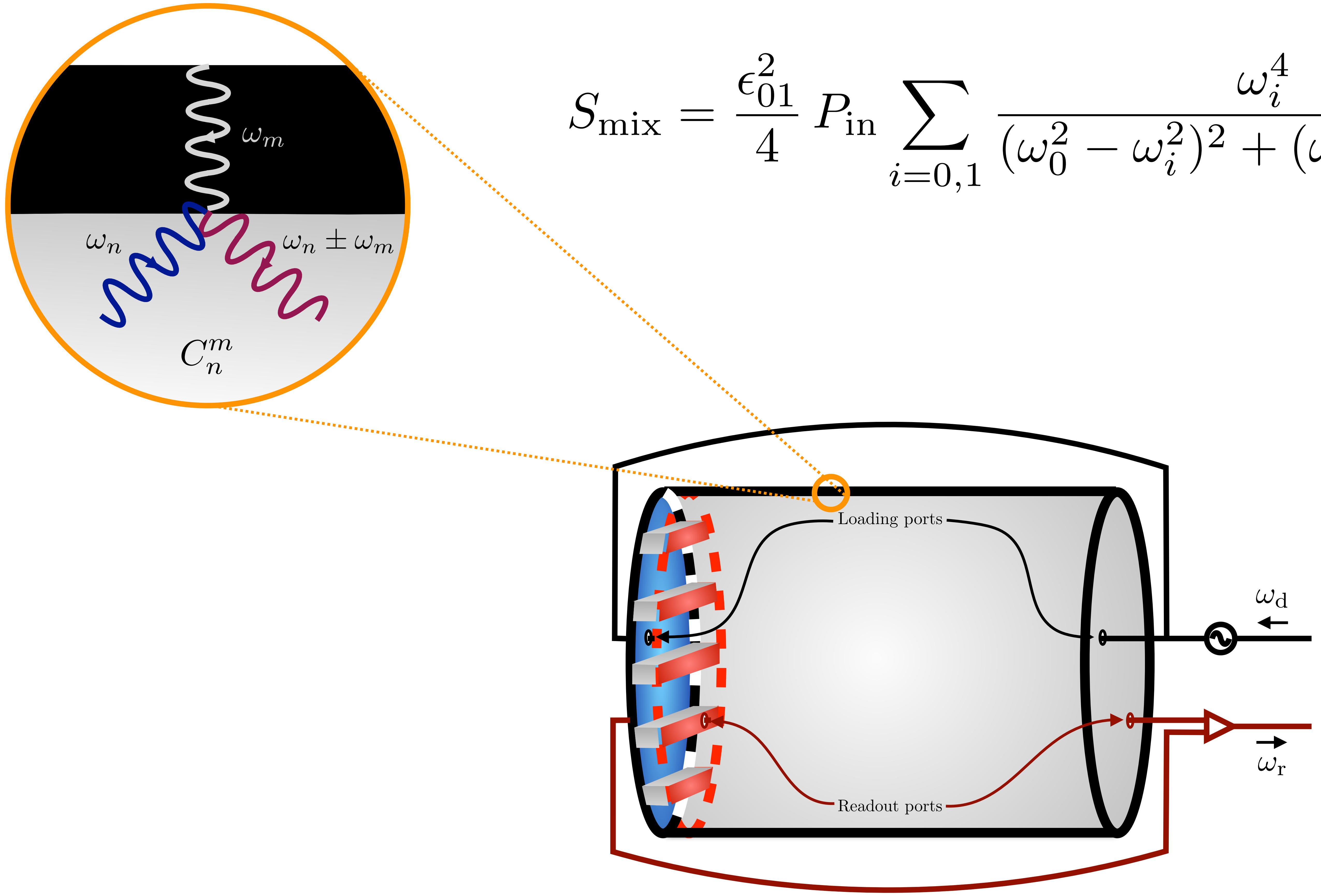

Power Spectral Density:

$$S_{\text{mix}} = \frac{\epsilon_{01}^2}{4} P_{\text{in}} \sum_{i=0,1} \frac{\omega_i^4}{(\omega_0^2 - \omega_i^2)^2 + (\omega_0\omega_i/Q_i)^2} \frac{(\omega\omega_i)^2}{(\omega^2 - \omega_i^2)^2 + (\omega\omega_i/Q_i)^2} |C_i^m|^2 S_{q_m}(\omega - \omega_0)$$

Displacement PSD:

$$S_{q_m}(\omega) \simeq \frac{1}{M^2} \frac{S_{f_m}(\omega)}{(\omega^2 - \omega_m^2)^2 + (\omega_m\omega/Q_m)^2}$$

Non-standard Noise Sources: Vibrations mixing

Vibrations

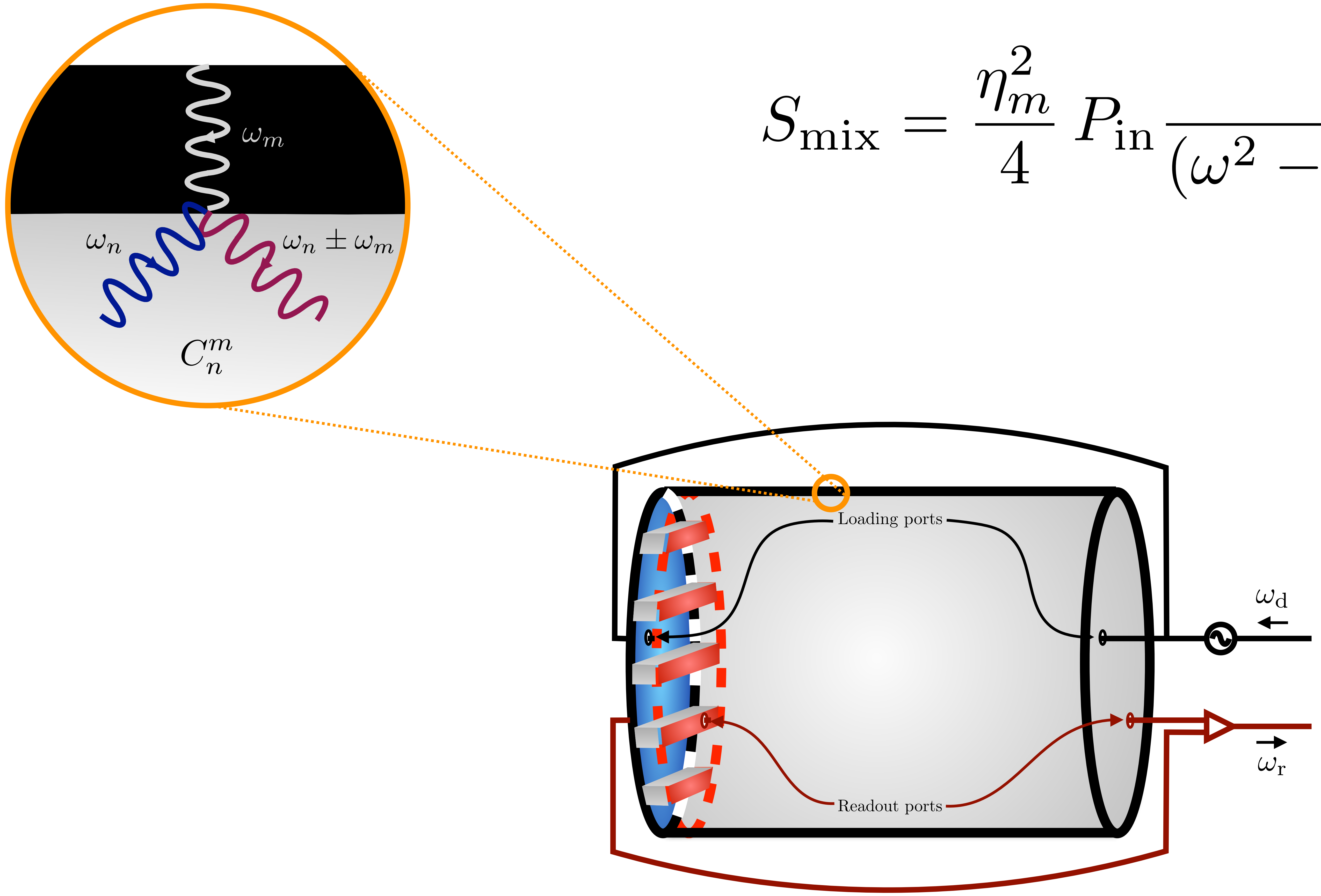

Power Spectral Density:

$$S_{\rm mix} = \frac{\eta_m^2}{4} P_{\rm in} \frac{\omega_0^4}{(\omega^2 - \omega_1^2)^2 + (\omega\omega_1/Q_1)^2} |C_1^m|^2 S_{q_m}(\omega - \omega_0)$$

Displacement PSD:

$$S_{q_m}(\omega) \simeq \frac{1}{M^2} \frac{S_{f_m}(\omega)}{(\omega^2 - \omega_m^2)^2 + (\omega_m \omega/Q_m)^2}$$

Non-standard Noise Sources: Field Emission

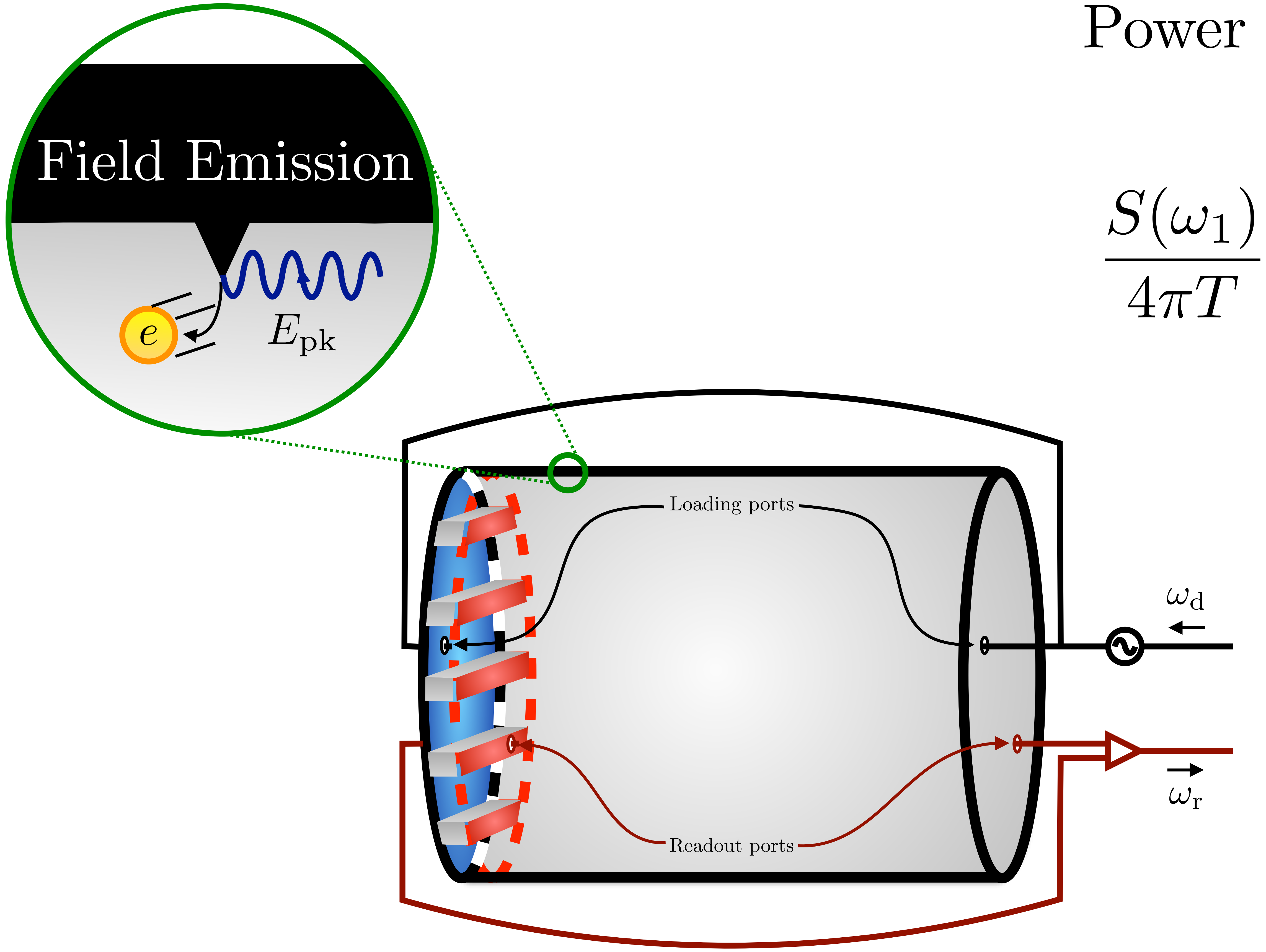

Power Spectral Density:

$$\frac{S(\omega_1)}{4\pi T} \sim \frac{P_{\rm tot}}{0.1\ \rm W} \times \begin{cases} 1 & \text{synchrotron} \\ 10^{-6} & \text{transition} \\ 10^{-5} & \text{Bremsstrahlung}\,, \end{cases}$$

Limits max B-field ~ 0.2 T

All Noise Sources

B = 0.1 T, T = 2K, $\omega_0 = 2\pi$ GHz, V = 0.05 m³

$$P_{\rm mech} \sim \epsilon_{\rm 1d}^2 \delta^2 \frac{\omega_0^2 \omega_{\rm min}^3}{m_a^5} P_{\rm in}$$

fractional wall disp. δ

$$P_{\rm mix} \sim \eta_m^2 \delta^2 \frac{Q_1 Q_m \omega_1 \omega_{\rm min}^3}{m_a^4} P_{\rm in}$$

$$P_{\rm th} \sim T \frac{\omega_1}{Q_{\rm int}}$$

$$P_{\rm phase} \sim \epsilon_{\rm 1d}^2 S_\varphi(m_a) \frac{\omega_1}{Q_{\rm int}} P_{\rm in}$$

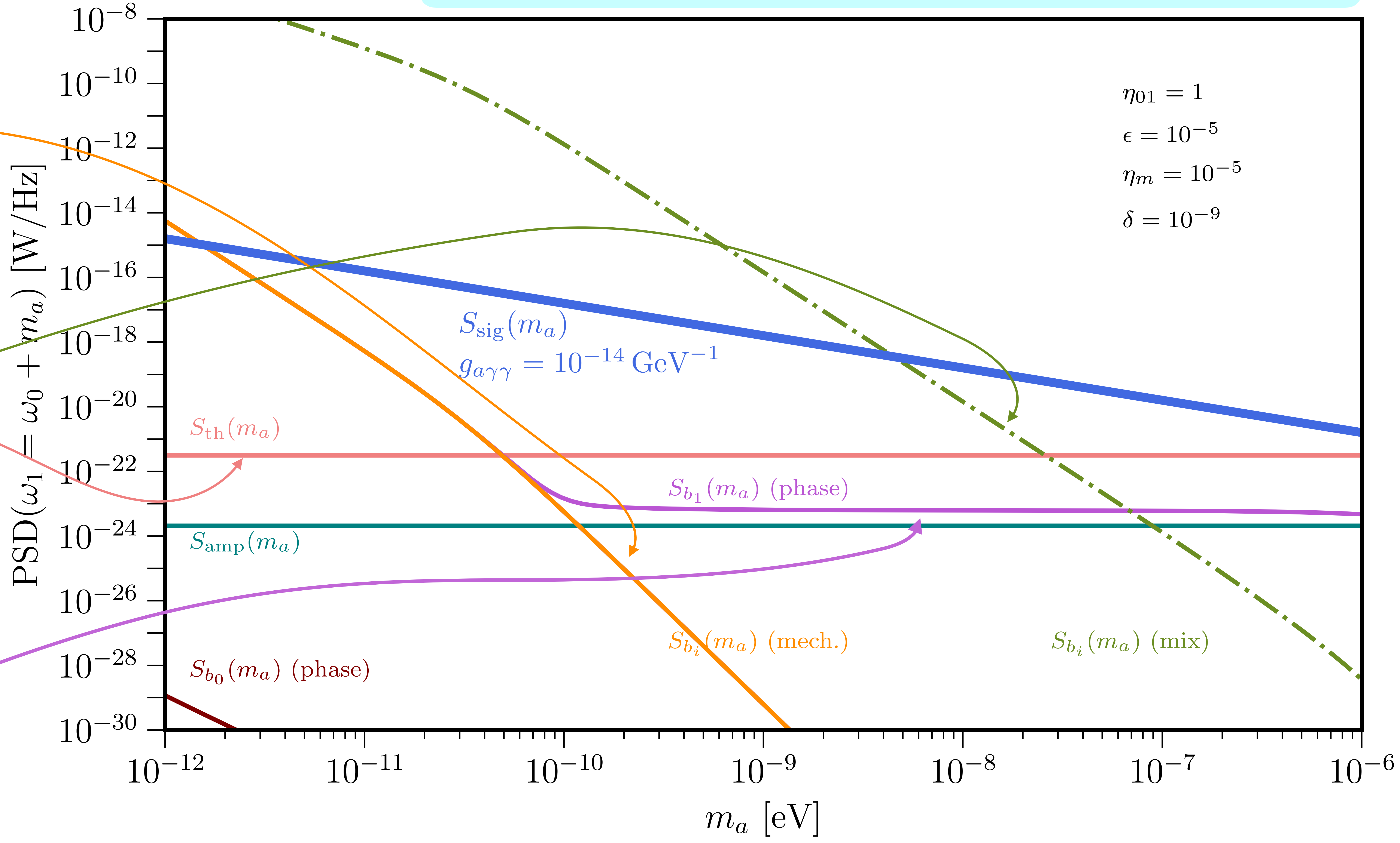

Technology Requirements

Q-factor & B-field:

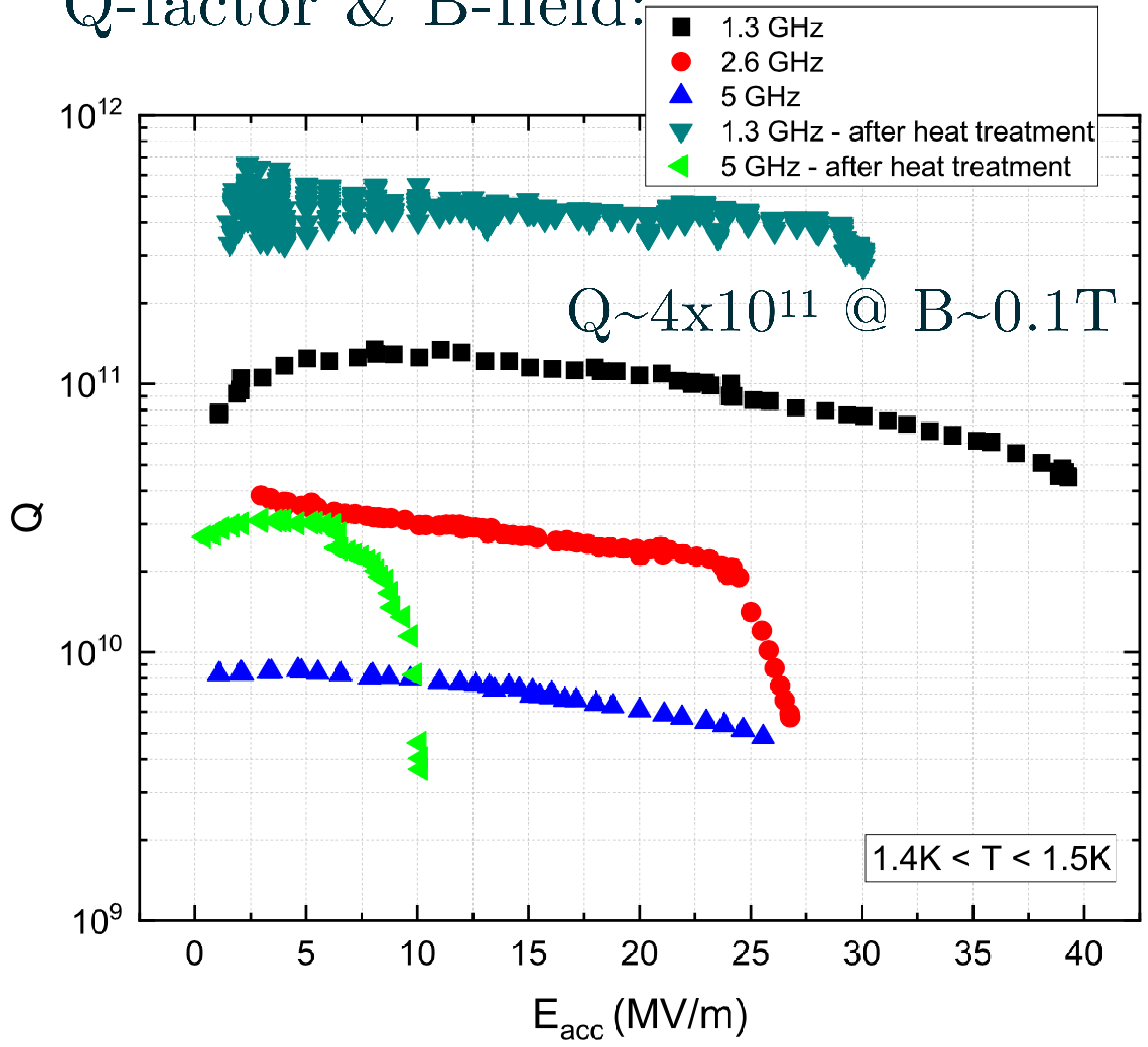

arXiv: 1810.03703 Romanenko et al.

Phase noise: *e.g.* BN865-M

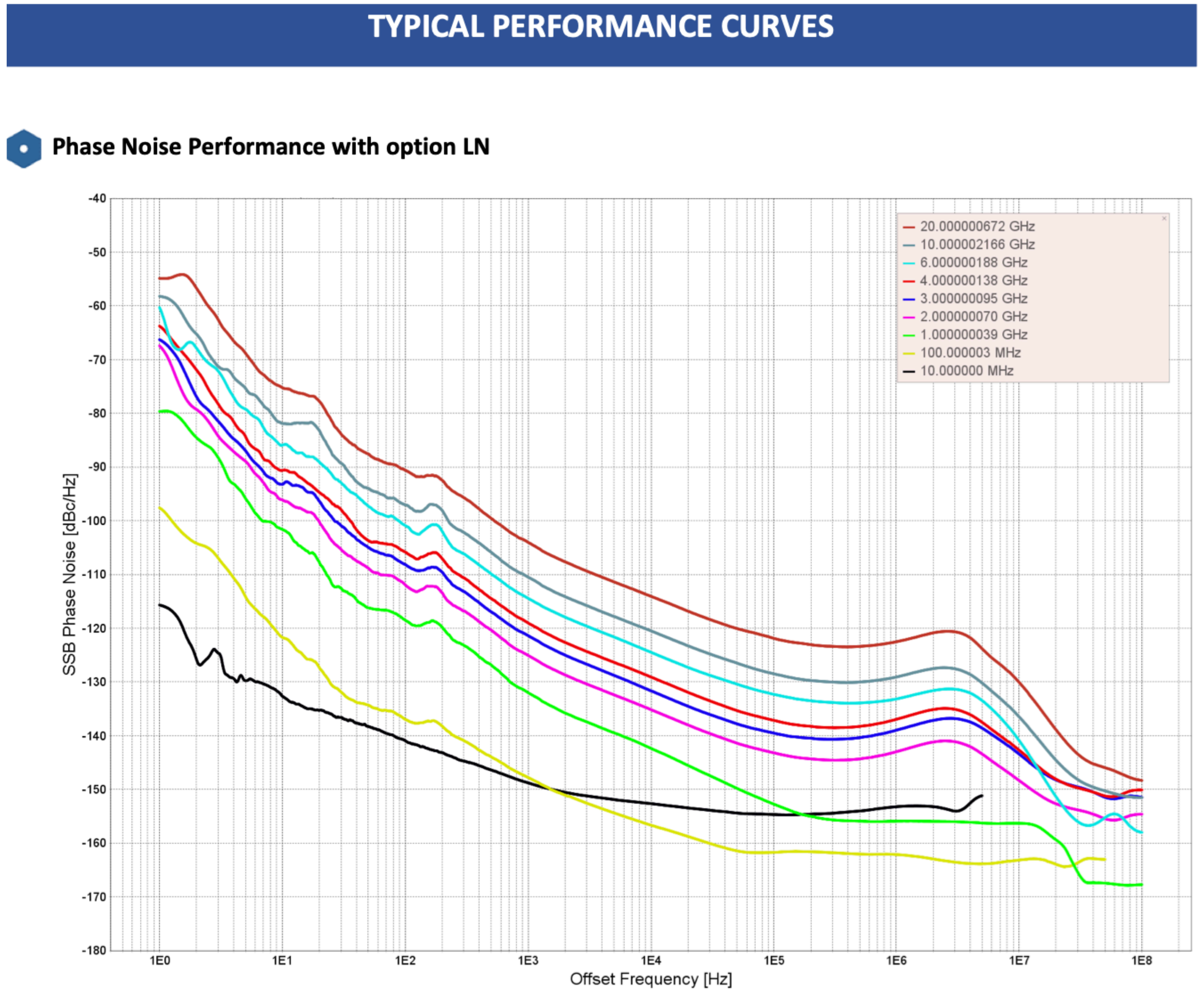

In total need ~ -240 dB/Hz @ GHz to reach thermal noise floor

Technology Requirements

Mode rejection:

$\epsilon = 10^{-7}$ achieved

gr-qc/0502054 Ballantini, ..., Calatroni et al
physics/0004031 Bernard, Gemme, Parodi, Picasso

Technology Requirements

Mode rejection:

$\epsilon = 10^{-7}$ achieved

Original MAGO collaboration

gr-qc/0502054 Ballantini, ..., Calatroni et al

physics/0004031 Bernard, Gemme, Parodi, Picasso

Technology Requirements

Mode rejection:

$\epsilon = 10^{-7}$ achieved

Original MAGO collaboration

gr-qc/0502054 Ballantini, ..., Calatroni et al

physics/0004031 Bernard, Gemme, Parodi, Picasso

Low-frequency seismic noise:

$$\Delta\omega/\omega \sim \delta \sim 10^{-10}$$

DarkSRF (2020)

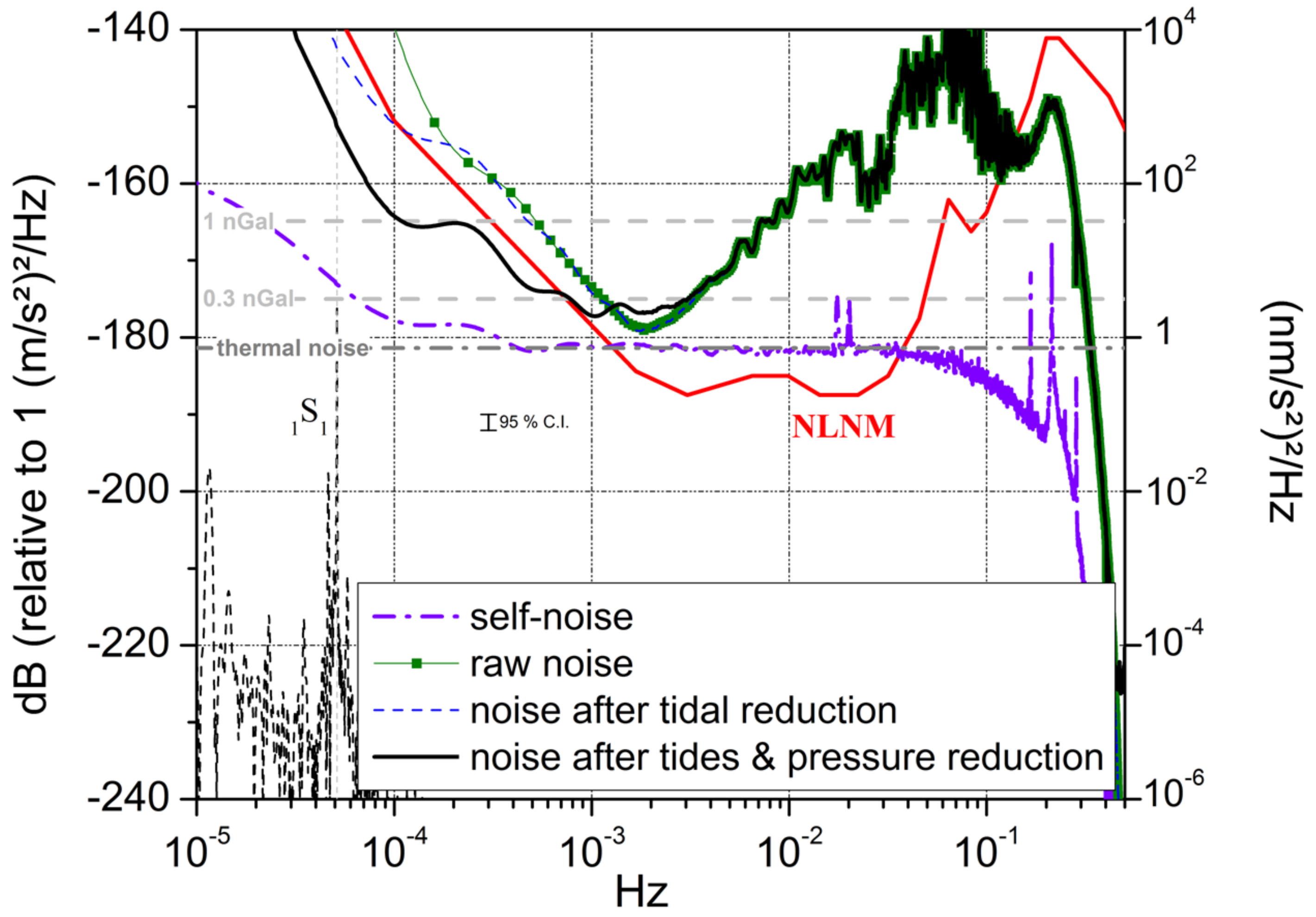

Scientific Reports 8, 15324 (2018) Rosat & Hinderer

Resonant Axion Resonant Frequency Conversion

B = 0.2 T, T = 2K, ω_0 = 1 GHz

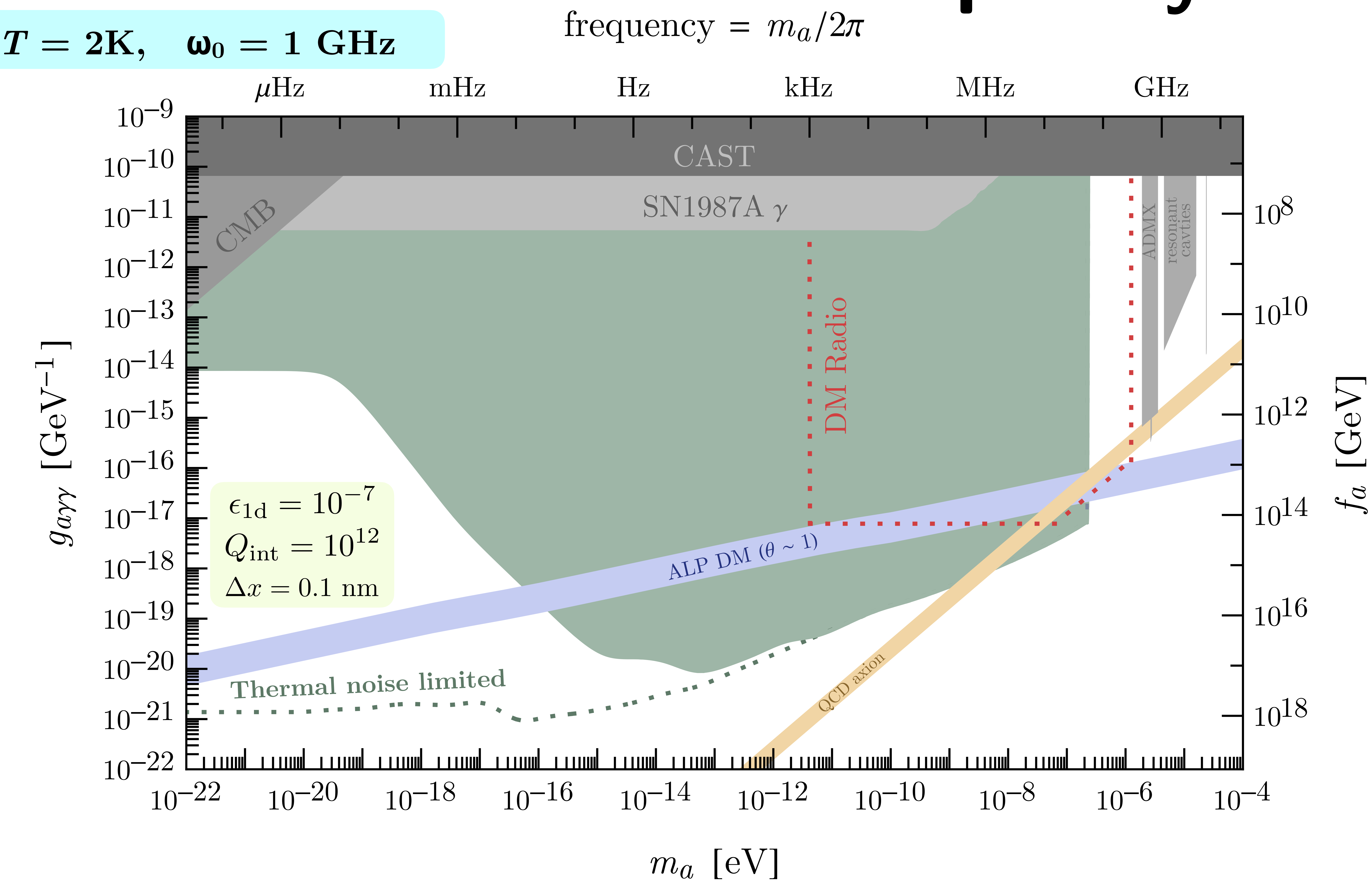

Resonant Axion Resonant Frequency Conversion

$\mathbf{B = 0.2\ T}, \quad \boldsymbol{T} \mathbf{= 2K}, \quad \boldsymbol{\omega_0} \mathbf{= 1\ GHz}$

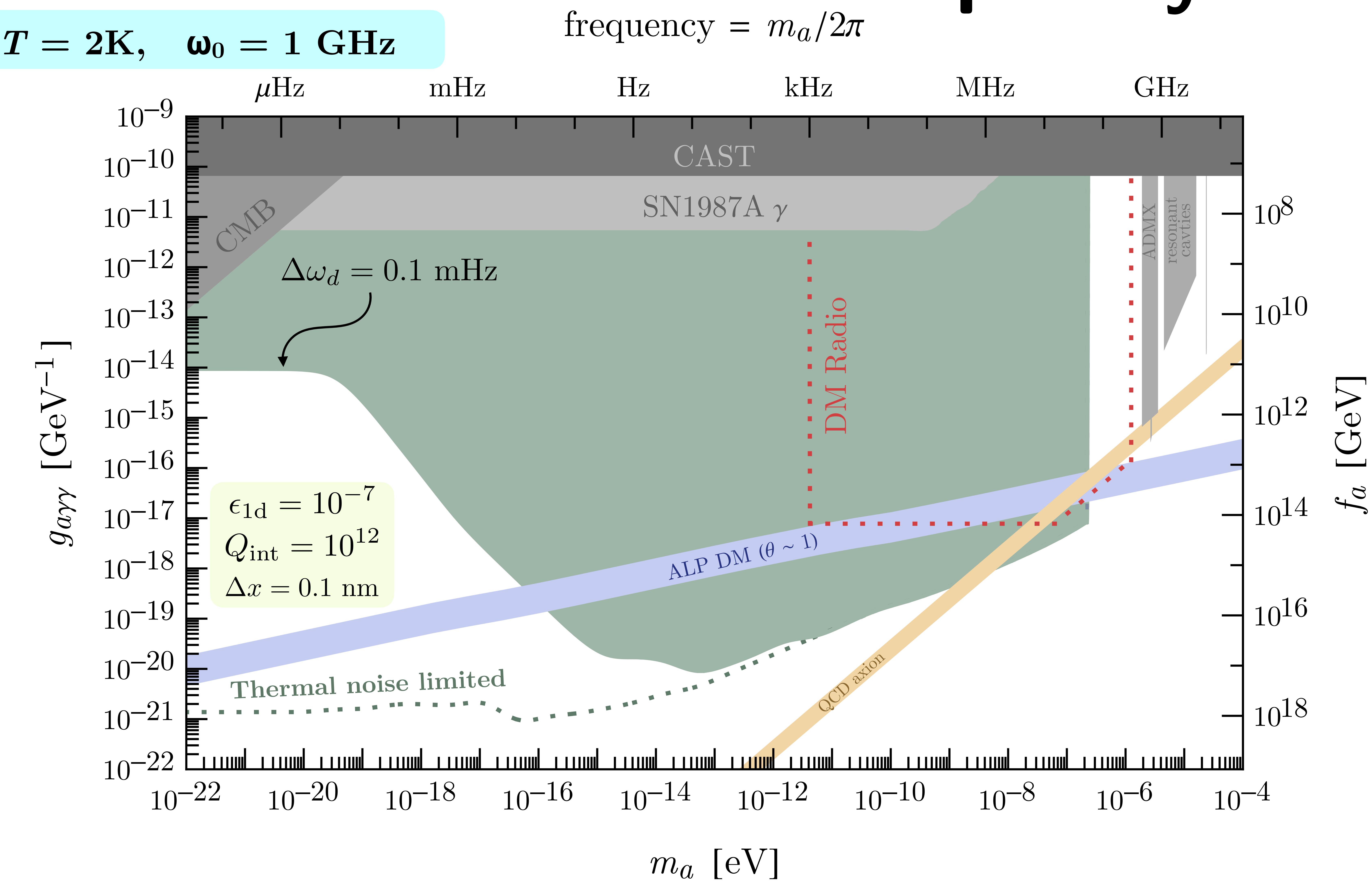

Resonant parameter variations: *Q-factor*

$\mathbf{B = 0.2\ T, \quad \mathit{T} = 2K, \quad \omega_0 = 1\ GHz}$

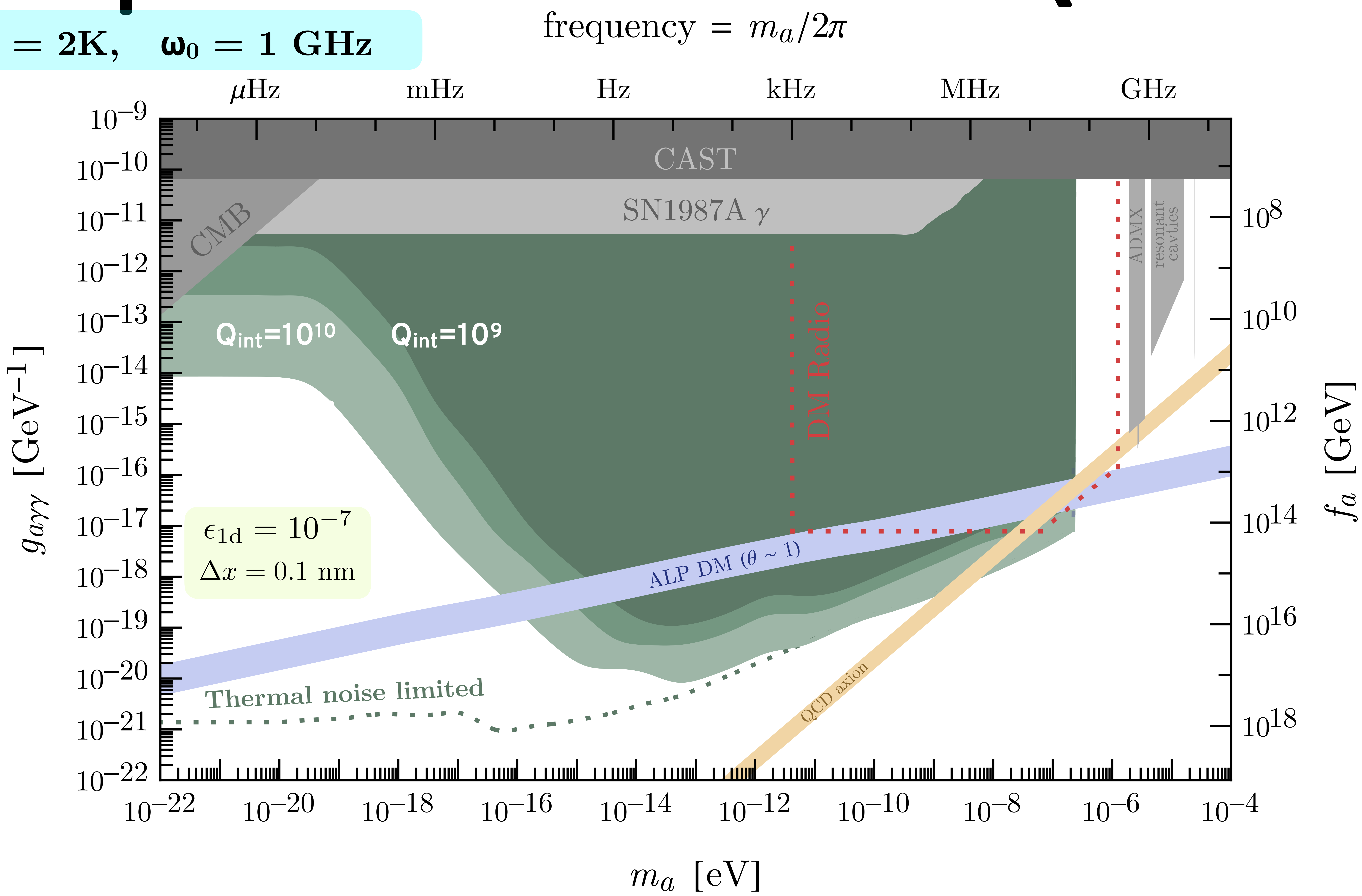

Resonant parameter variations: *mode rejection*

$\mathbf{B = 0.2\ T, \quad \mathit{T} = 2K, \quad \omega_0 = 1\ GHz}$

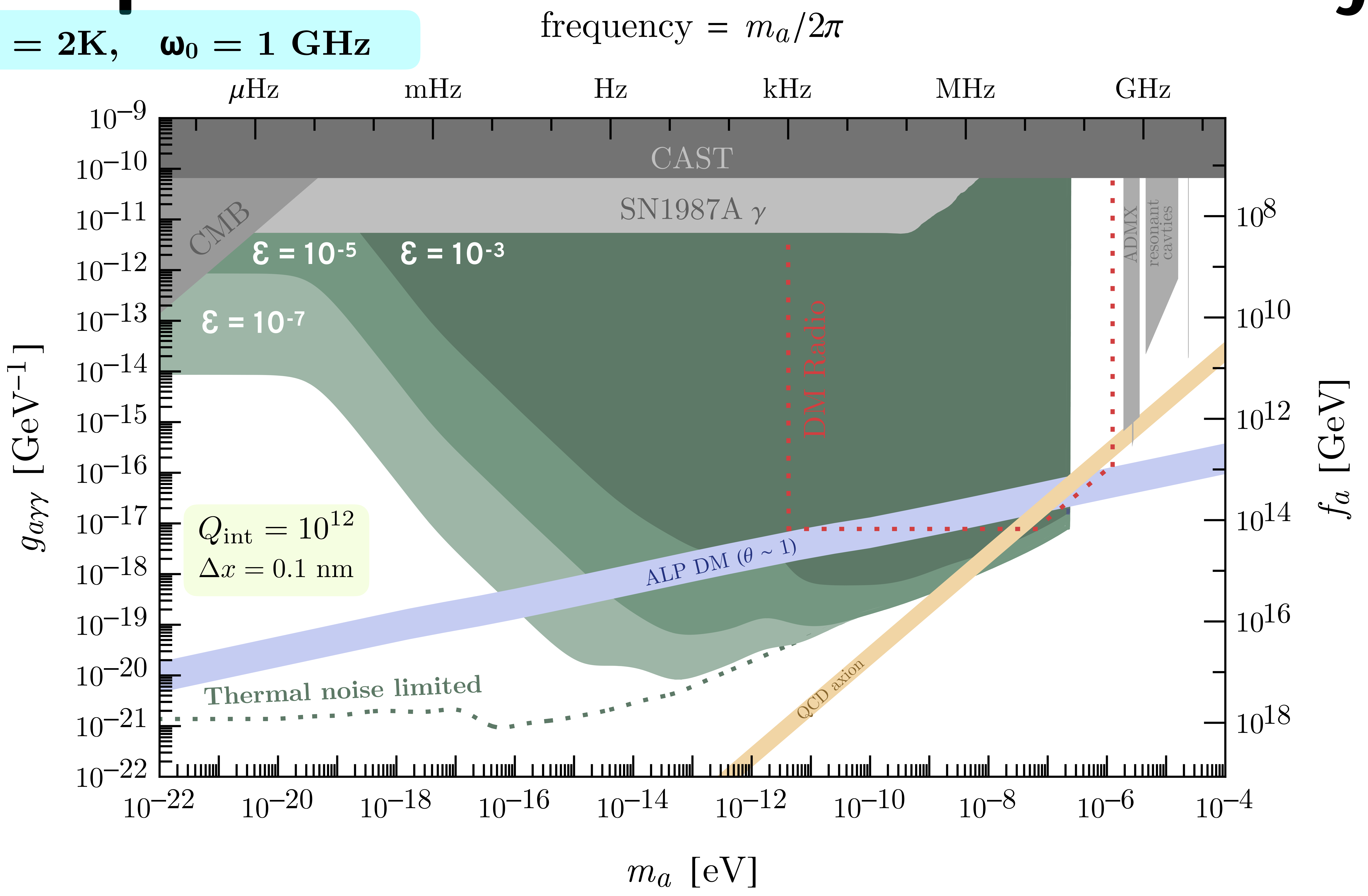

Resonant parameter variations: *mode rejection*

$B = 0.2$ T, $T = 2$K, $\omega_0 = 1$ GHz